(some) Observed properties of moist convection on earth

Adam Sobel

FDEPS Kyoto

Outline

1. Marine boundary layer – stratocumulus to trade cumulus transition
2. Deep convection
3. Climatology of precipitation and related quantities

Moist boundary layer over ocean

Adam Sobel
FDEPS Kyoto

Klein et al. (1995, *J. Climate*) – satellite image of Scu-Cu transition – visible reflectance from satellite

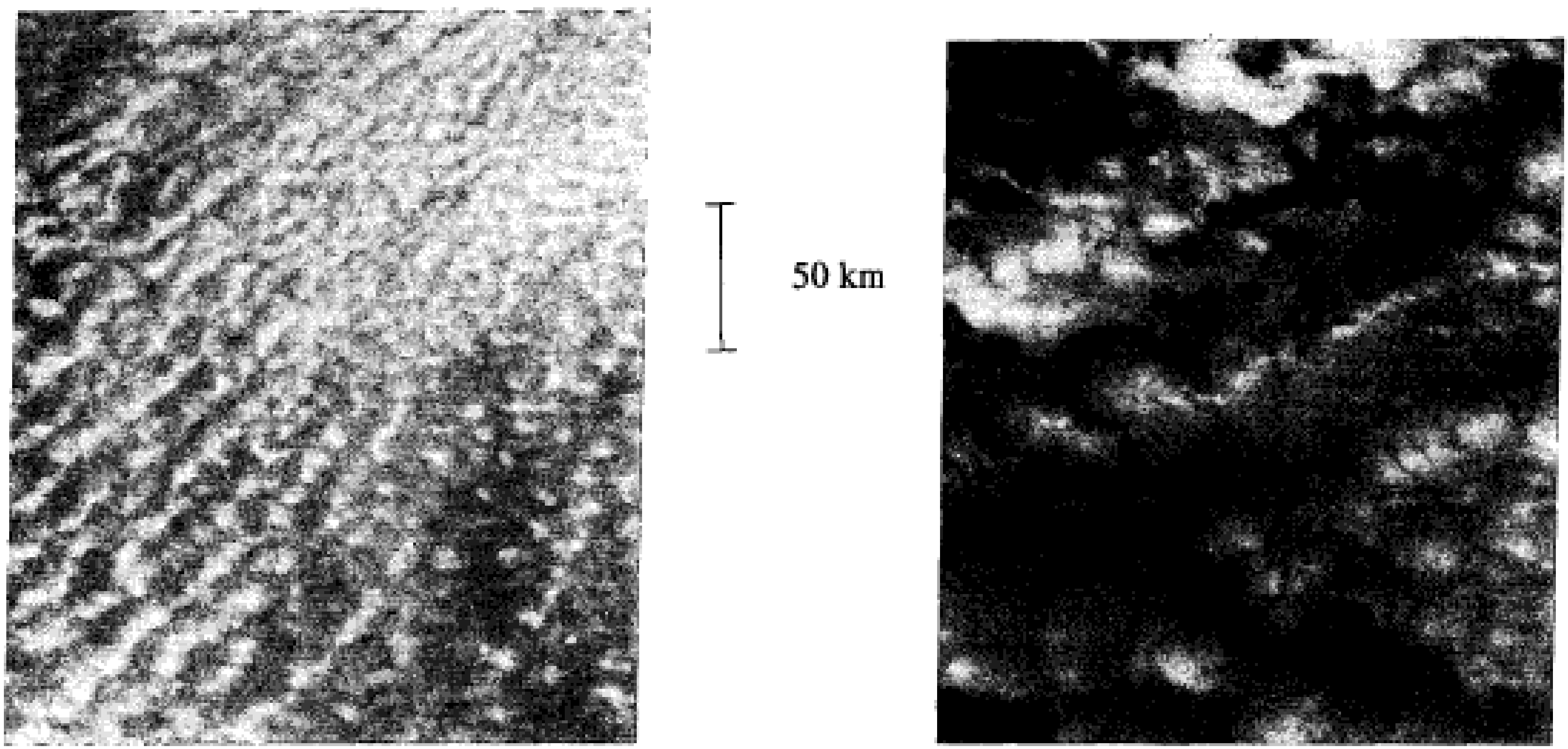

35N

30N, downstream

Klein et al. (1995, *J. Climate*) – satellite image of Scu-Cu transition – visible reflectance from satellite

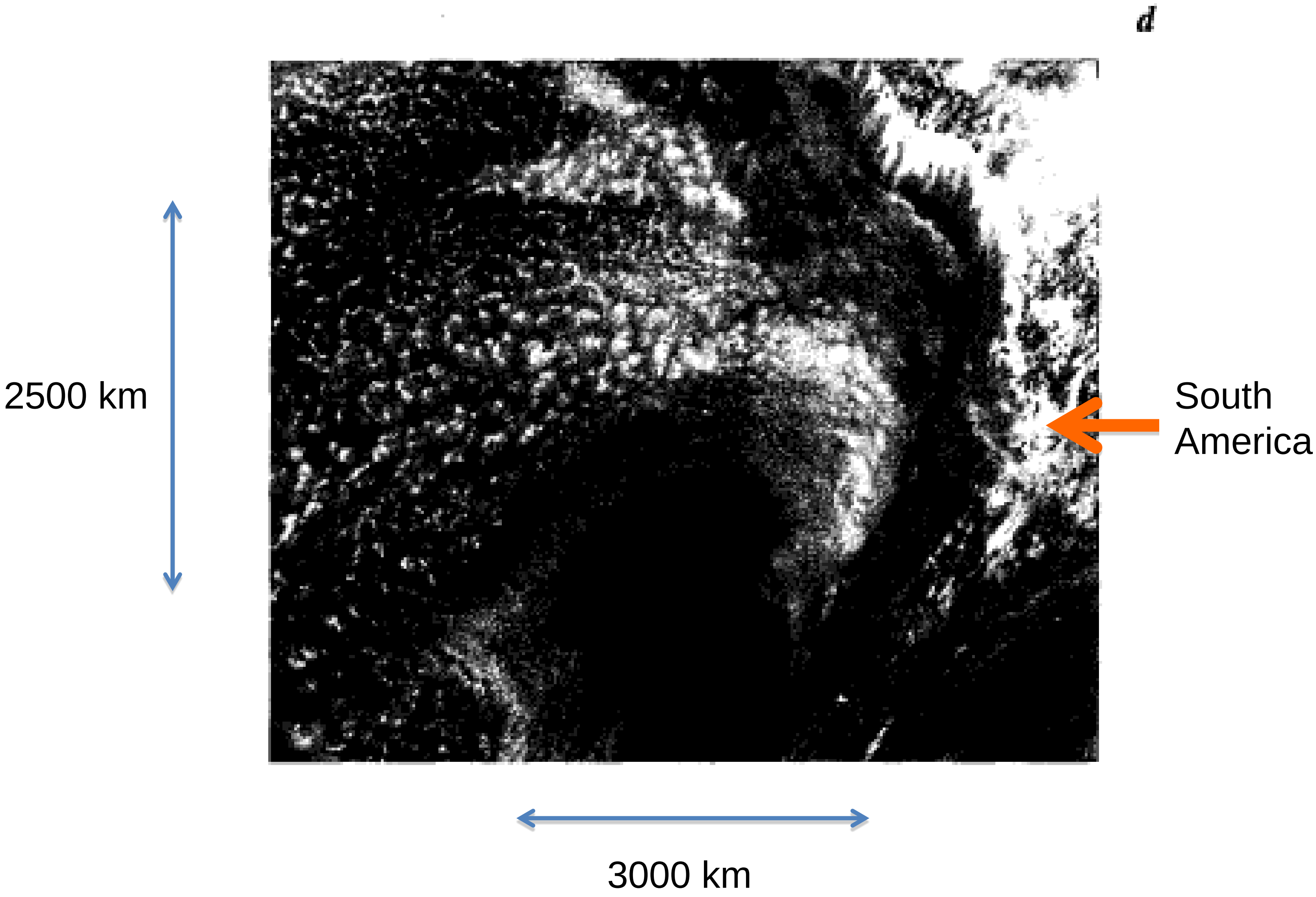

Klein et al. (1995, *J. Climate*) – climatological frequencies of stratocumulus and cumulus

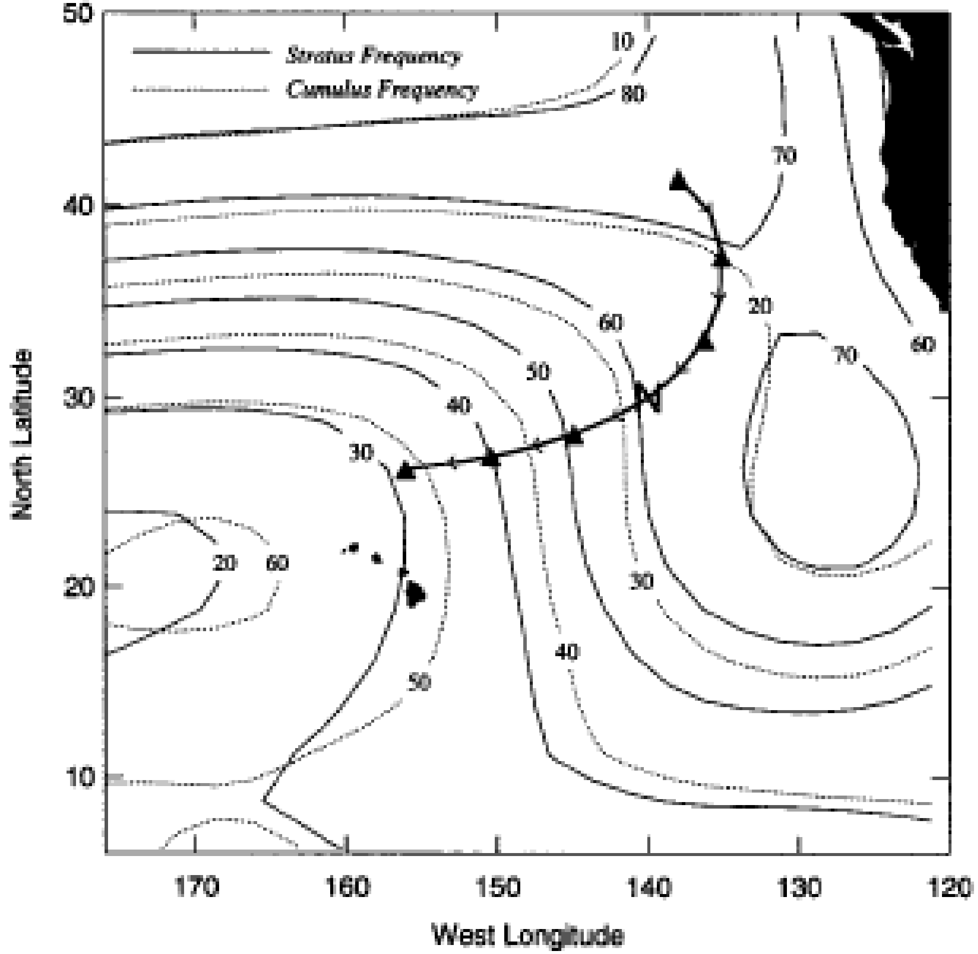

FIG. 2. Mean June–July–August frequency of stratus, stratocumulus, or fog (solid lines) and cumulus (dotted lines) clouds from the compilations of ship observations by Warren et al. (1988). This climatology is based upon data from the years 1952–81.

Schematic of stratocumulus-topped marine boundary layer (Stevens, 2006, *Theor. Comp. Fluid Dyn.)* – layer is well-mixed, turbulence is driven largely by radiative cooling at cloud top

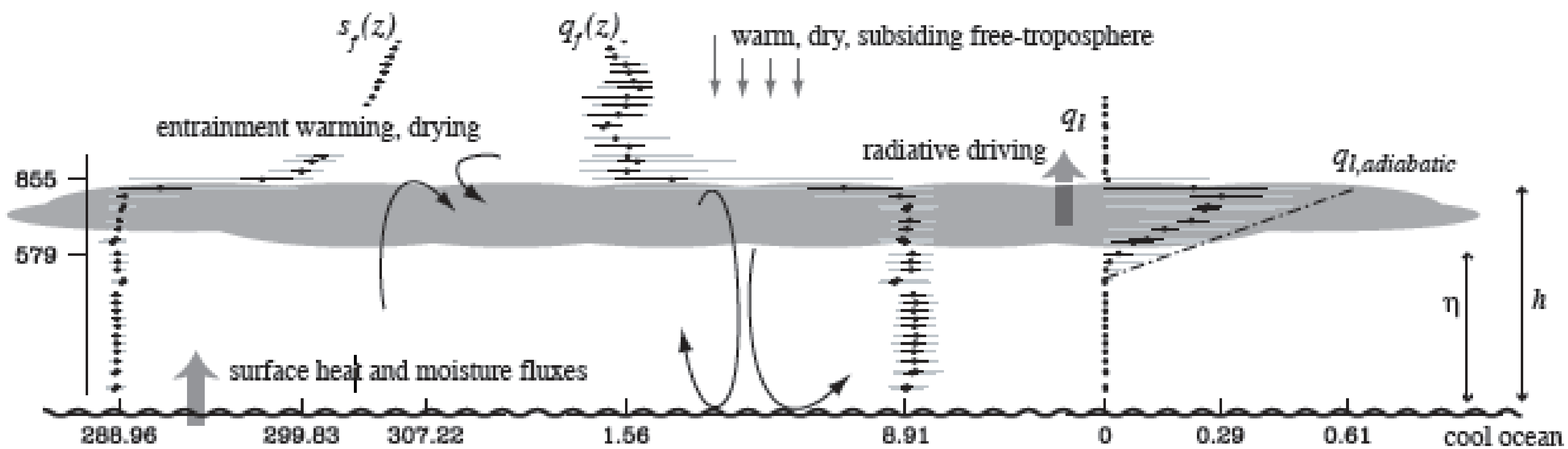

Fig. 1 Structure of the stratocumulus topped boundary layer as observed during DYCOMS-II.

Composite shallow Cu boundary layers, from Albrecht et al. (1995, *JGR*)

FIRE – SCu
ASTEX – SCu/Cu transition
TIWE – Trade Cu

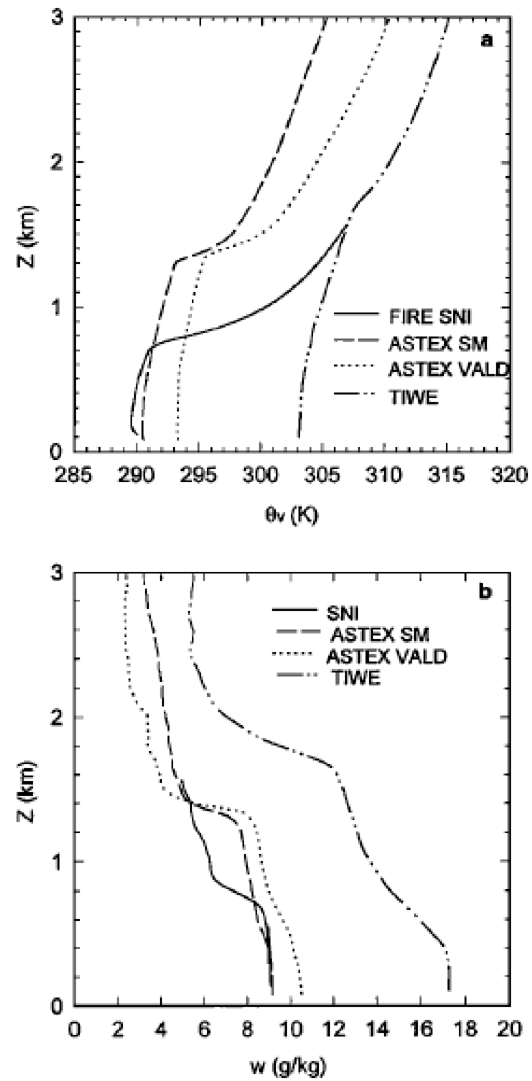

Composite soundings normalized by inversion height, z_i

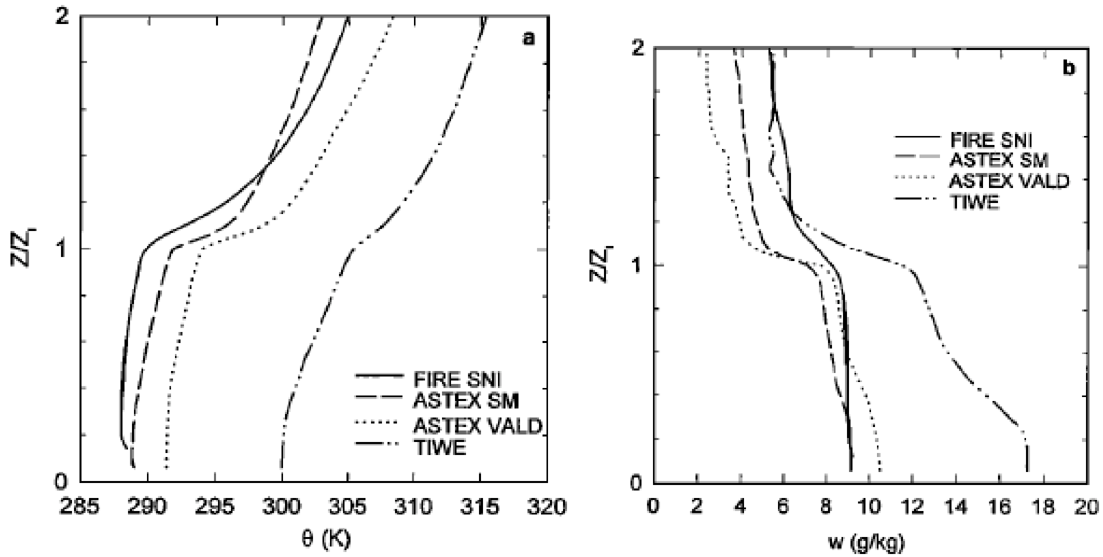

Figure 1. Composite vertical profiles of (a) potential temperature and (b) mixing ratio for San Nicolas Island, Santa Maria, R/V *Valdivia*, and Tropical Instability and Waves Experiment using height scales normalized by the height of the inversion.

Albrecht et al. (1995, *JGR*)

Relative humidity

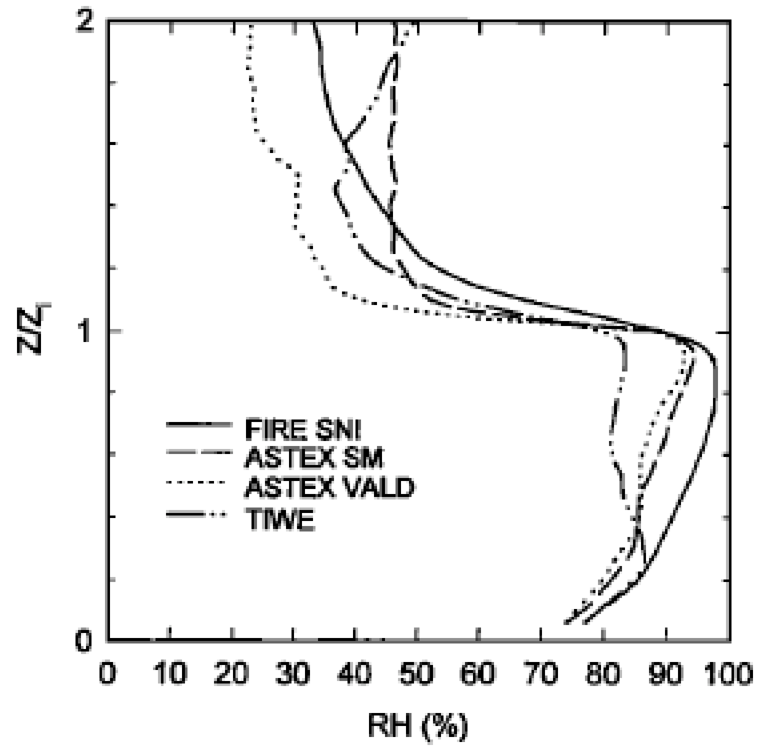

Figure 3. Same as Figure 1 but for relative humidity.

Albrecht et al. (1995, *JGR*)

μ_e, μ_e^*

Note shallow layer of conditional instability $d\theta_{es}/dz<0$, and sfc θ_e larger than Upper θ_{es}

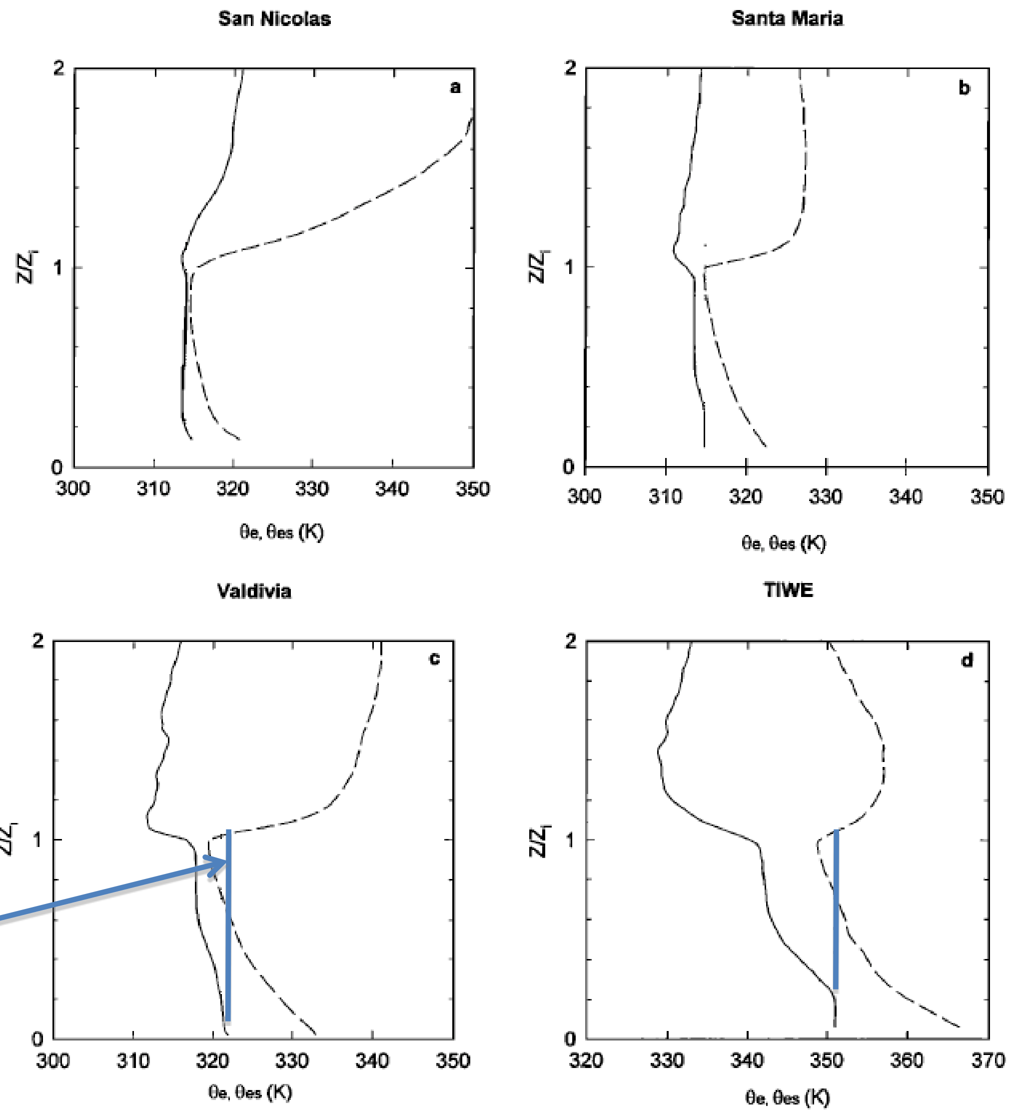

Figure 4. Composite profiles of θ_e (solid curve) and θ_{es} (dashed curve) for the four data sets. The dotted curve shows the θ_e path of a parcel originating from z/z_i = 0.2.

Albrecht et al. (1995, *JGR*)

Scu – Trade Cu transition

- Stratocumulus is well mixed in both μ_v and q – somewhat closer to dry convection, just with saturated layer at top (since q* drops with height while q~const)
- As surface warms and buoyancy increases, cumuli start to punch deeper; we see increasingly stable and dry layer form
- Entrainment of dry air from above eventually dries out SCu layer

E.g., Wyant et al. 1997, *J. Atmos. Sci.* 54, 168

Wyant et al. (~~1999~~ 1997, *J. Atmos. Sci.*): Lagrangian LES simulations of column moving over increasingly warm water

μ_v

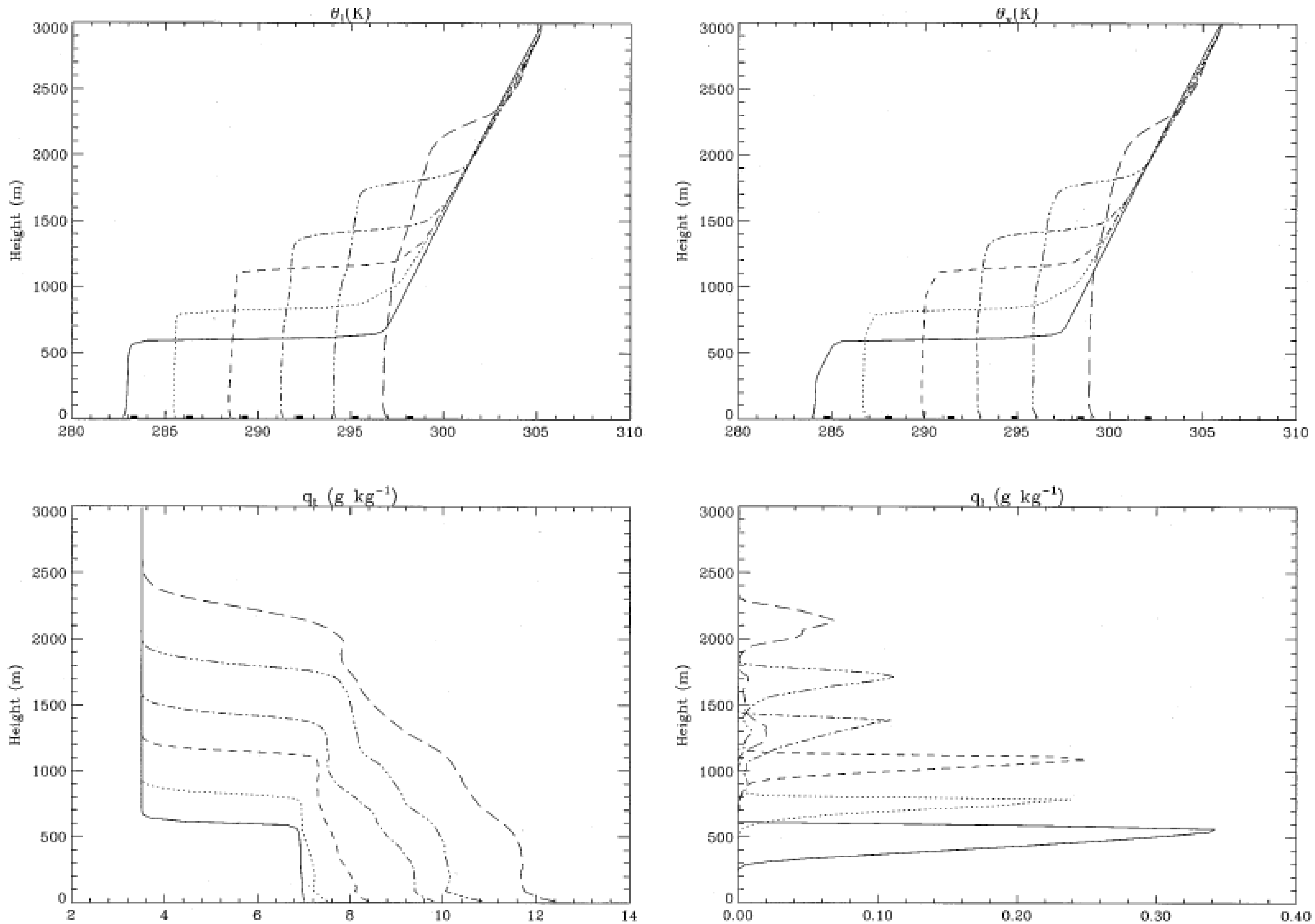

q_t q_l

Wyant et al. (1997, *J. Atmos. Sci.*): Lagrangian LES simulations of column moving over increasingly warm water

μ v

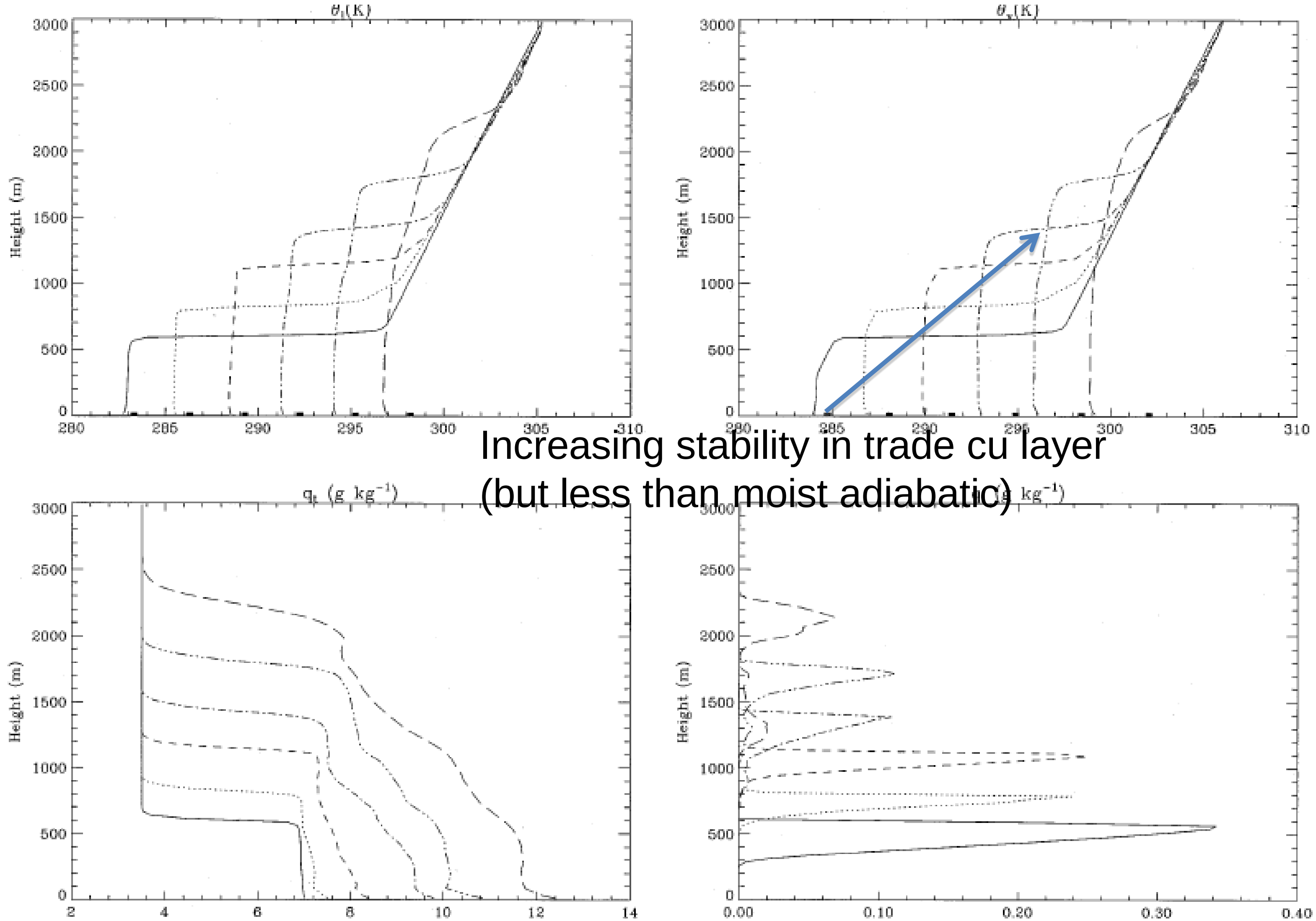

Increasing stability in trade cu layer
(but less than moist adiabatic)

q_t

q_l

Wyant et al. (1997, *J. Atmos. Sci.*): Lagrangian LES simulations of column moving over increasingly warm water

μ_v

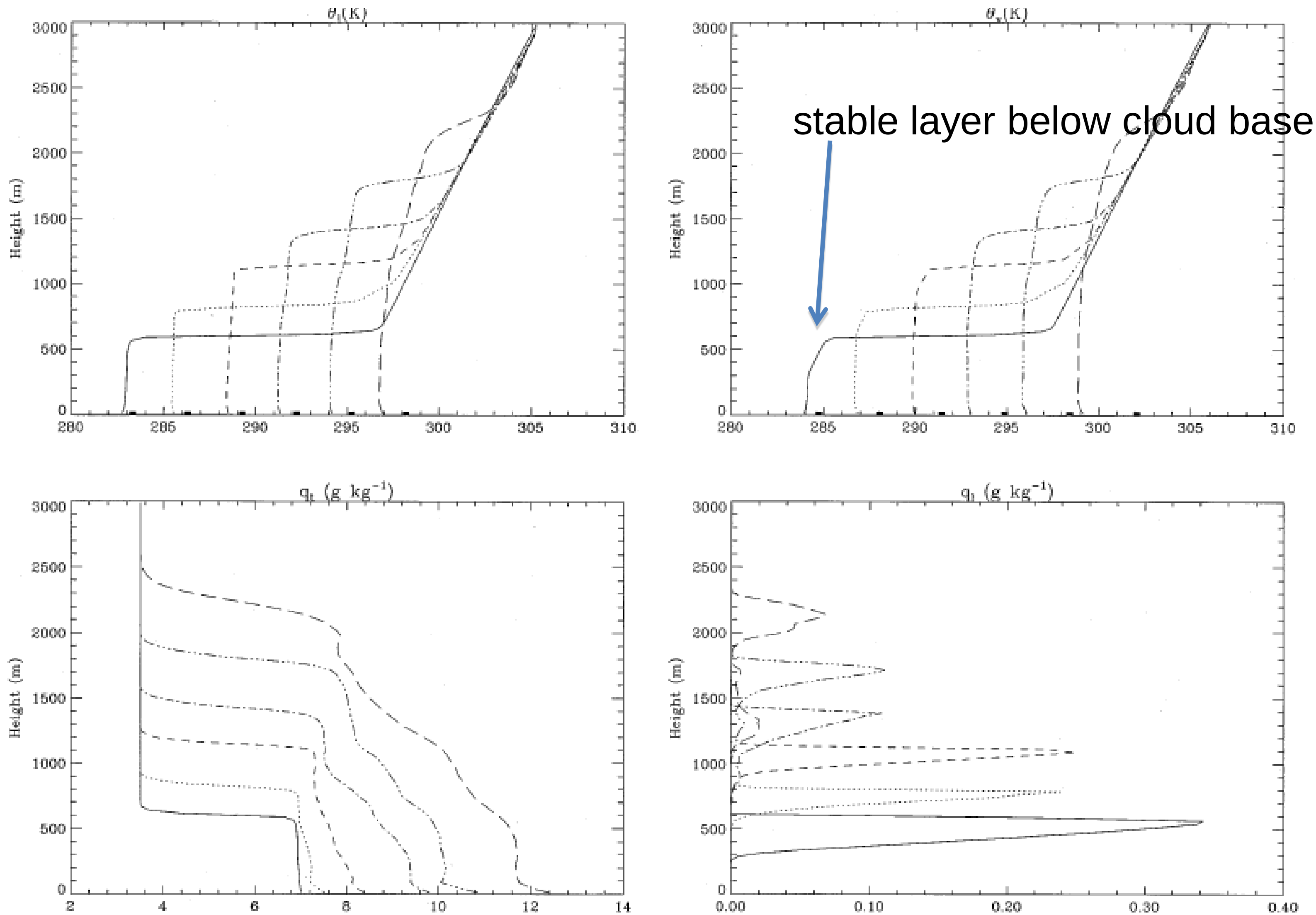

q_t q_l

Step 1 (Wyant et al. 1997):

“As SST warms and the MBL deepens, upward latent heat fluxes in the boundary layer increase dramatically. This increases the buoyancy fluxes and turbulence levels within the cloud, creating more entrainment per unit of cloud radiative cooling. The increased entrainment leads to increasingly negative buoyancy fluxes below cloud base associated with a downward flux of warm entrained air. This disrupts the mixed layer and creates a weak stable layer … below cloud base.
The stable layer acts as a valve that allows only the most powerful subcloud-layer updrafts to penetrate up to the main stratocumulus cloud base.
As the decoupling becomes more pronounced, the updrafts resemble small cumuli.”

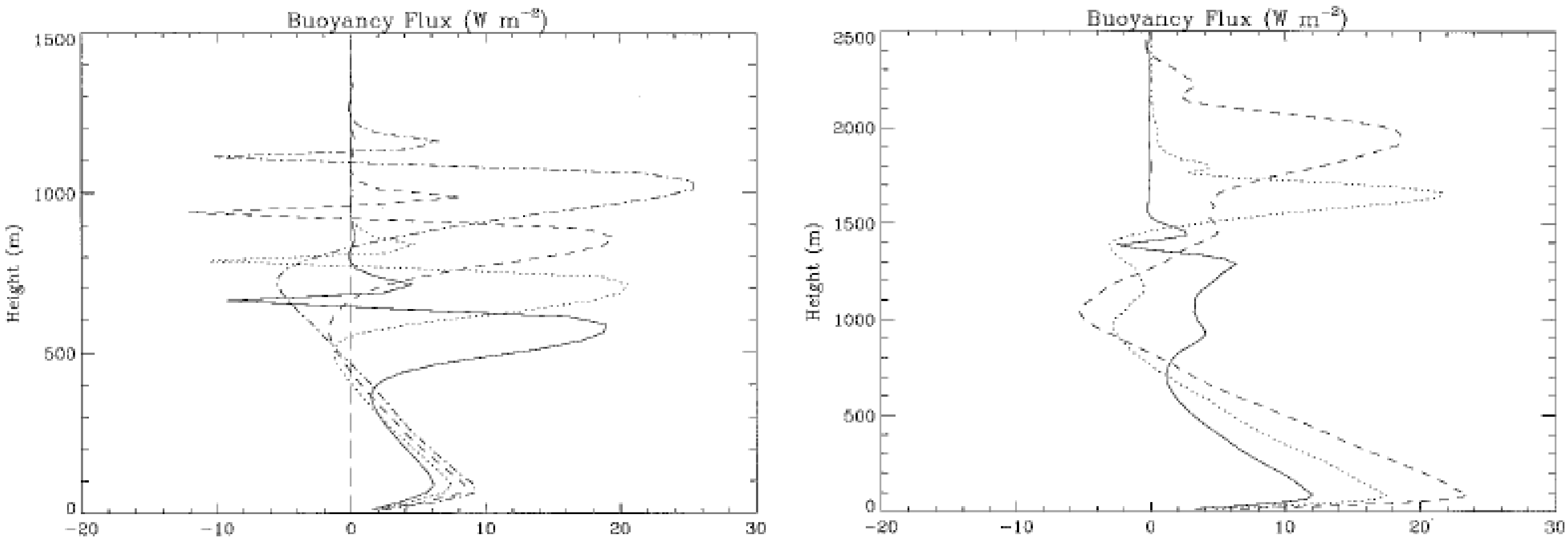

FIG. 5. Buoyancy flux profiles (2-h mean) in Cbase: (a) day 1 (solid), day 2 (dotted), day 3 (dashed), and day 4 (dashed–dotted) [A line is plotted along zero buoyancy flux (dashed) for reference]; (b) day 6 (solid), day 8 (dotted), and day 10 (dashed).

Wyant et al. (1997, *J. Atmos. Sci.*)

Step 2 (Wyant et al. 1997):

“While the cumulus clouds sustain the stratocumulus by detrainment of liquid water near the inversion, we suggest that they also cause its ultimate demise. Within the cumulus layer, the stratification is much weaker than moist adiabatic, so conditional available potential energy (CAPE) builds up rapidly as the cumulus layer deepens. … penetrative entrainment of dry free tropospheric air by increasingly vigorous cumulus clouds evaporates most of the liquid water in the updraft before it is detrained, leaving smaller and smaller stratocumulus cloud patches around the cumulus. The ratio of penetratively entrained mass flux of dry air to upward cumulus mass flux of moist surface-layer air increases, drying the cloud layer.”

Wyant et al. (1997, *J. Atmos. Sci.*)

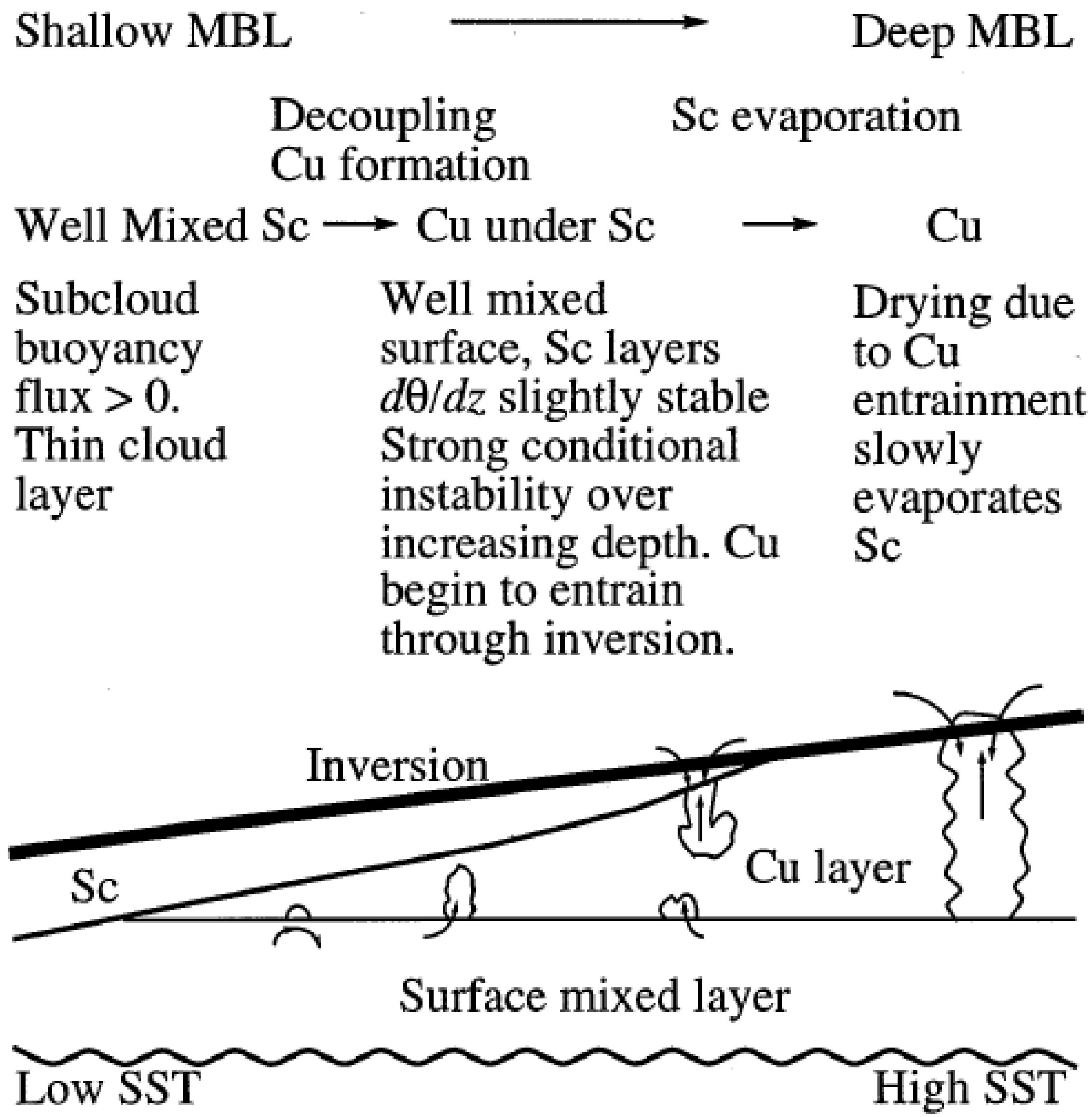

Deep Convection

Adam Sobel
FDEPS Kyoto

When sea surface is warm enough (relative to atmosphere) deep, strongly precipitating convection occurs

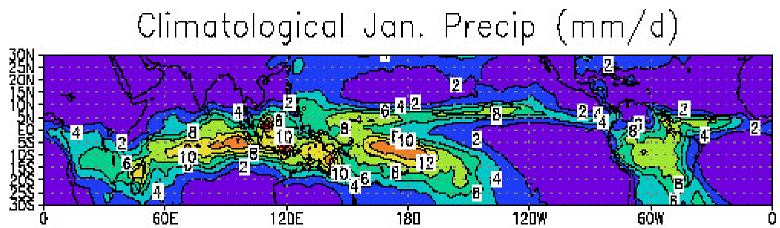

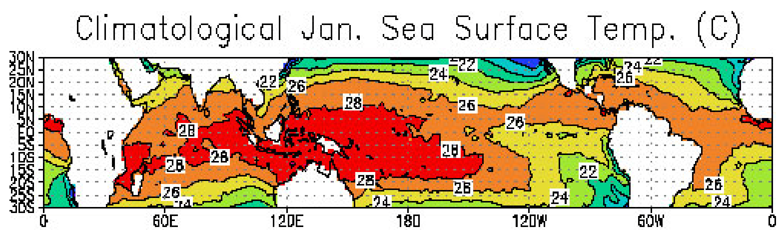

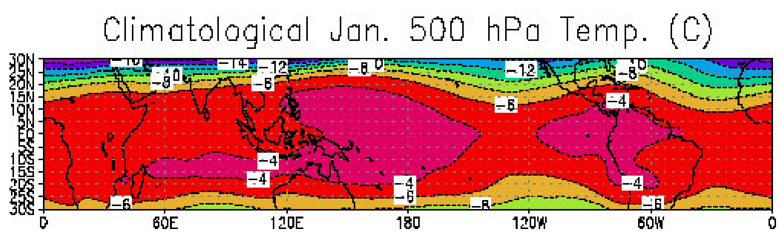

Seasonal cycle of precip follows the SST, which (very broadly) follows the sun, with a lag of a couple months

January

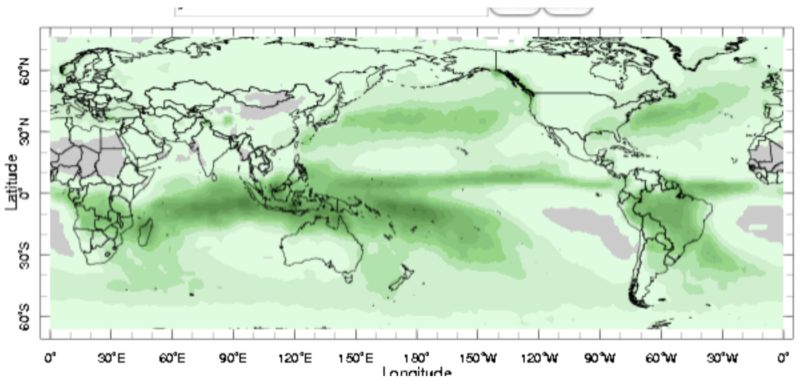

April

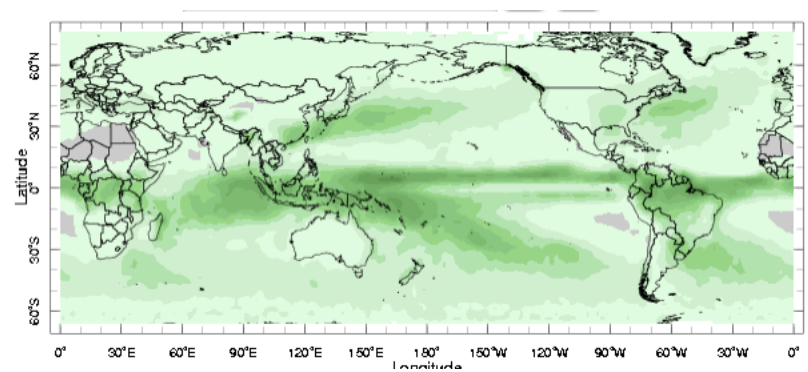

July

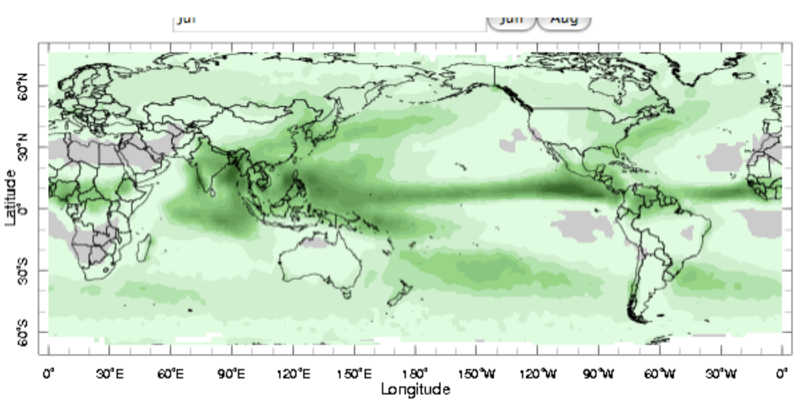

October

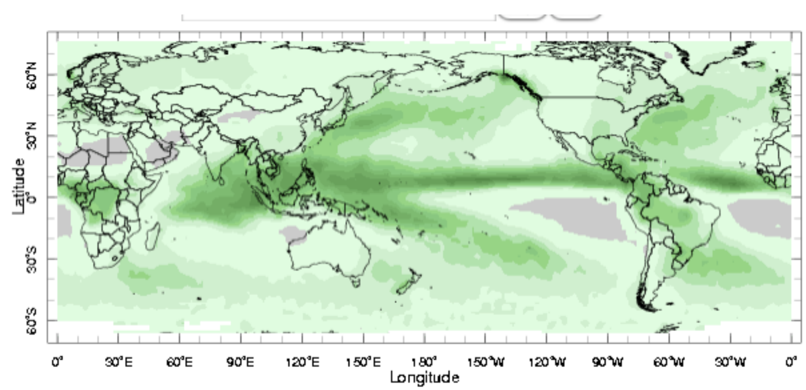

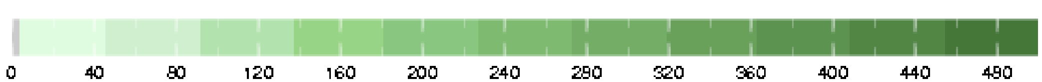

CMAP Monthly Precipitation Climatology (1979-2004 Base Period) [mm/month]

http://iridl.ldeo.columbia.edu/maproom/.IFRC/.Forecasts/

The deep convection is there because of conditional instability

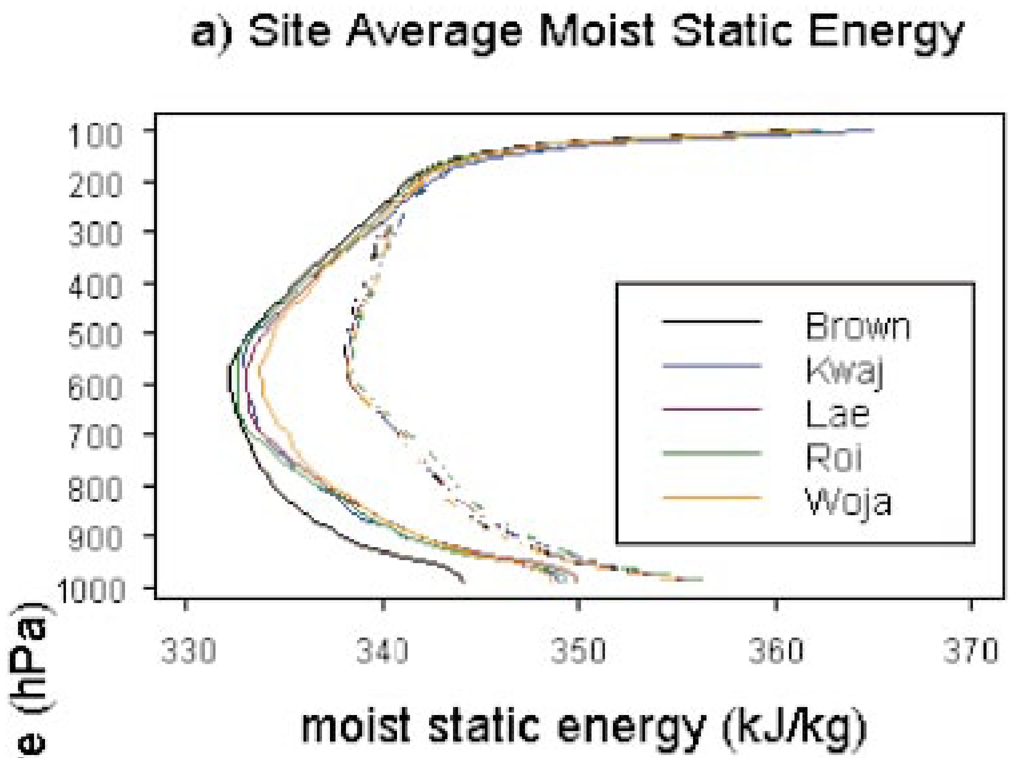

Sobel et al. 2004, *Mon. Wea. Rev*
KWAJEX field expt., Marshall Islands

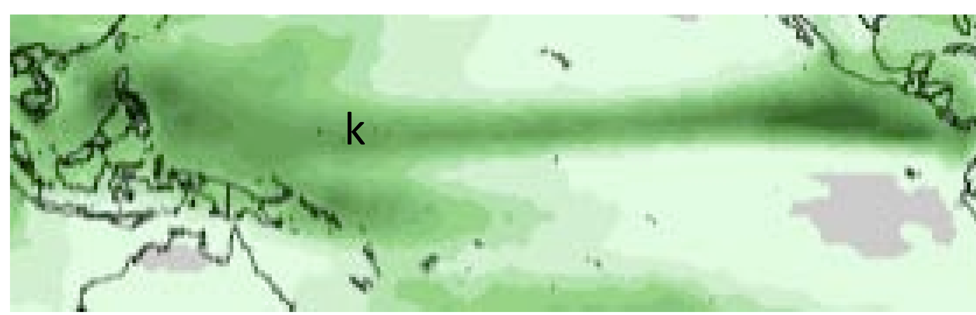

July precip climatology

Relative humidity doesn't show strong drop at PBL top. PBL not even that well defined (no inversion) though there is still a shallow mixed layer where RH increases with height (q ~ const)

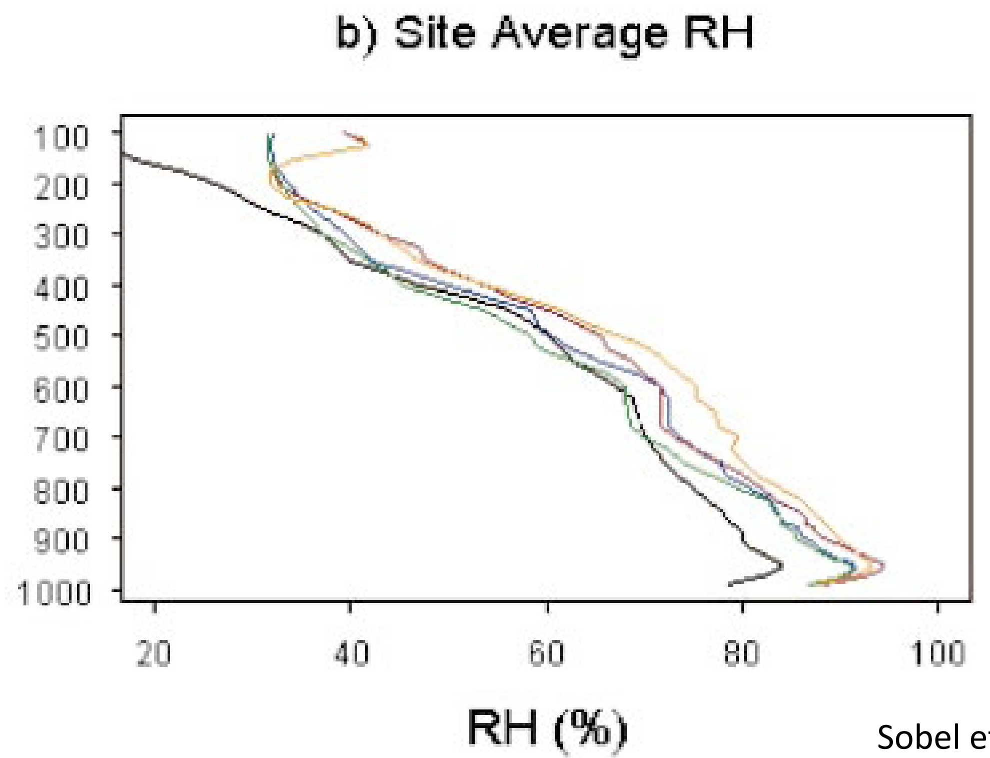

Sobel et al. 2004, Mon. Wea. Rev

Day-to-day variability in temperature is small, in humidity is larger

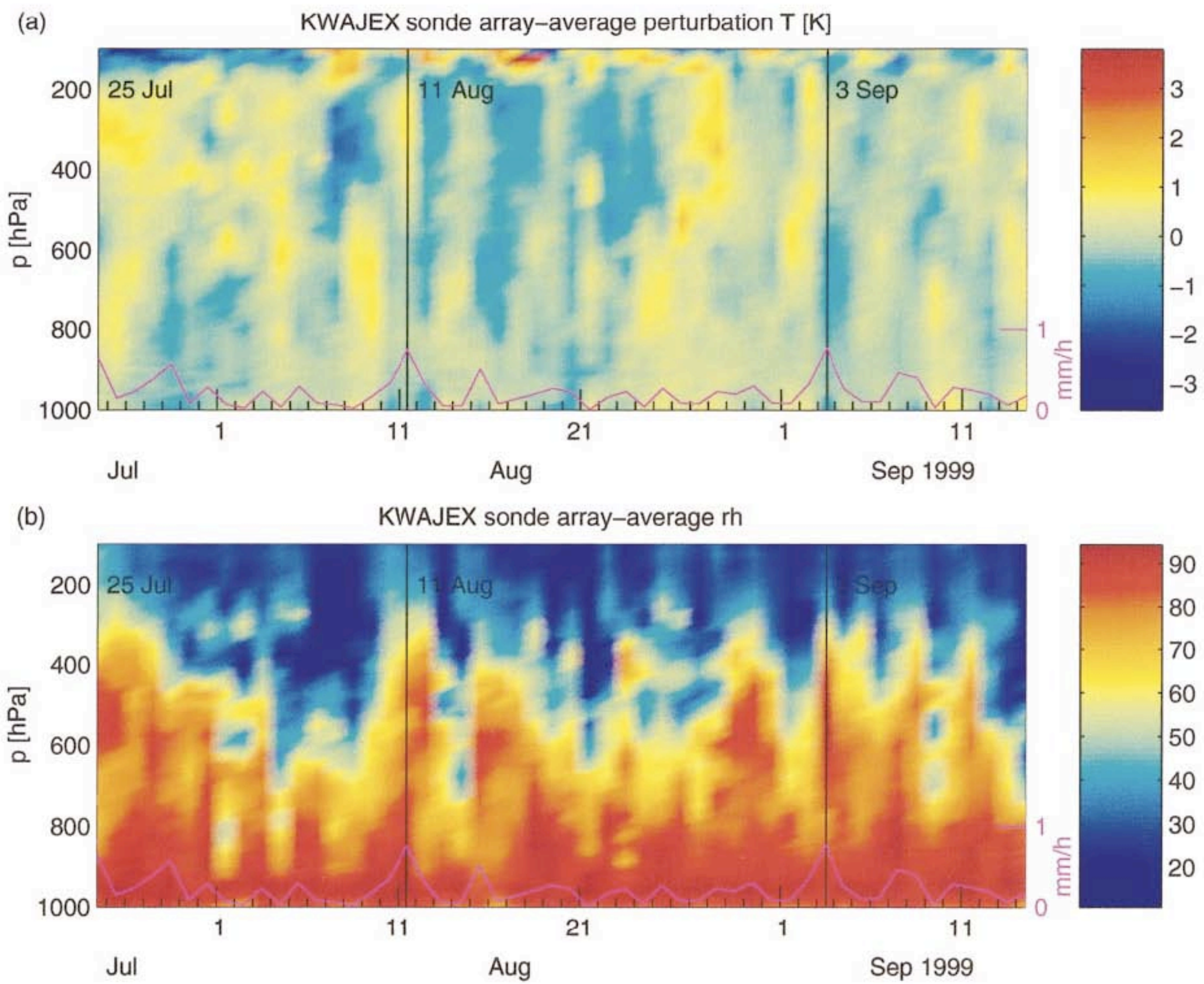

FIG. 8. Time–height plot of rawinsonde daily mean array averages during KWAJEX: (a) temperature perturbation, (b) relative humidity (with respect to liquid water), (c) u, and (d) v. Time series of daily mean rain rate (mm h^{-1}) is superimposed at the bottom of each plot, and vertical lines indicate 25 Jul, 11 Aug, and 3 Sep, the times of the three events discussed in detail in section 3.

Sobel et al. 2004, Mon. Wea. Rev

Much of the variability is related to coherent propagating large-scale disturbances

Black-body temperature (cold = high clouds = deep convection)

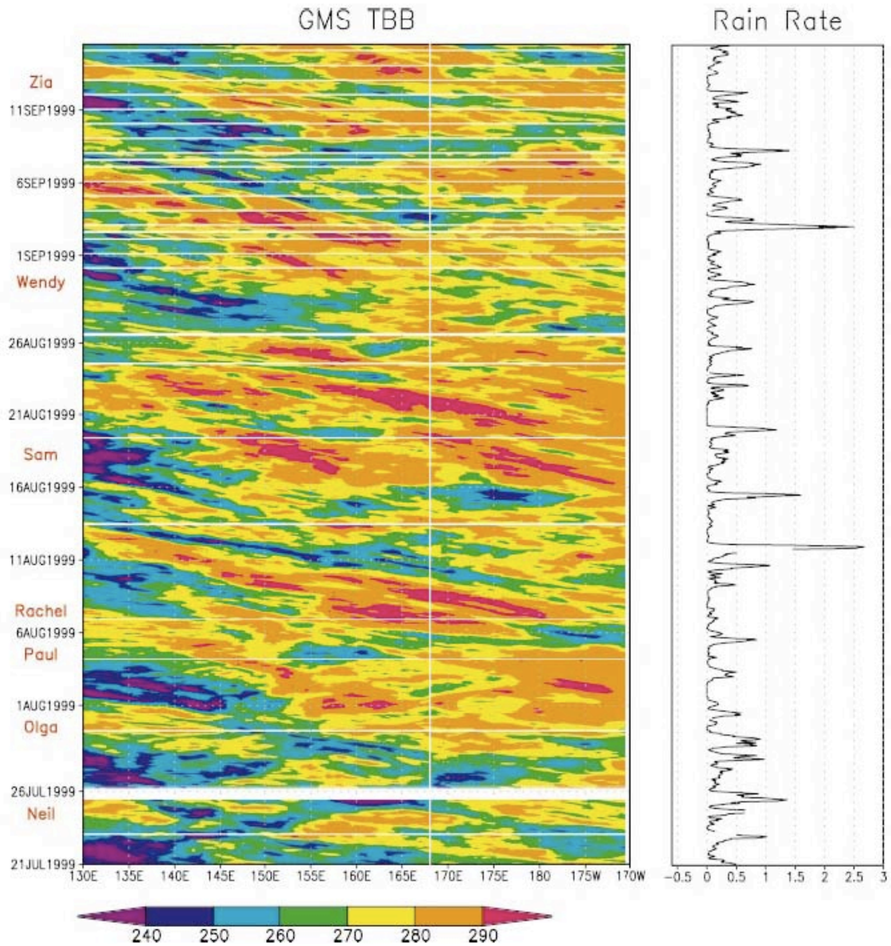

Time ->

Radar rain rate
From a ~200 km
Radius around
Kwajalein (white
Line)

FIG. 4. (left) GMS T_{BB} (K) averaged from 0°–15°N, as a function of time and longitude. (right) Time series of hourly and areally averaged rain rate (mm h^{-1}) from the Kwajalein radar. Vertical white line indicates longitude of Kwajalein, and words in red at left indicate tropical cyclones; see text for details.

Sobel et al. 2004, Mon. Wea. Rev

Longitude ->

Many different morphologies and degrees and kinds of space-time organization

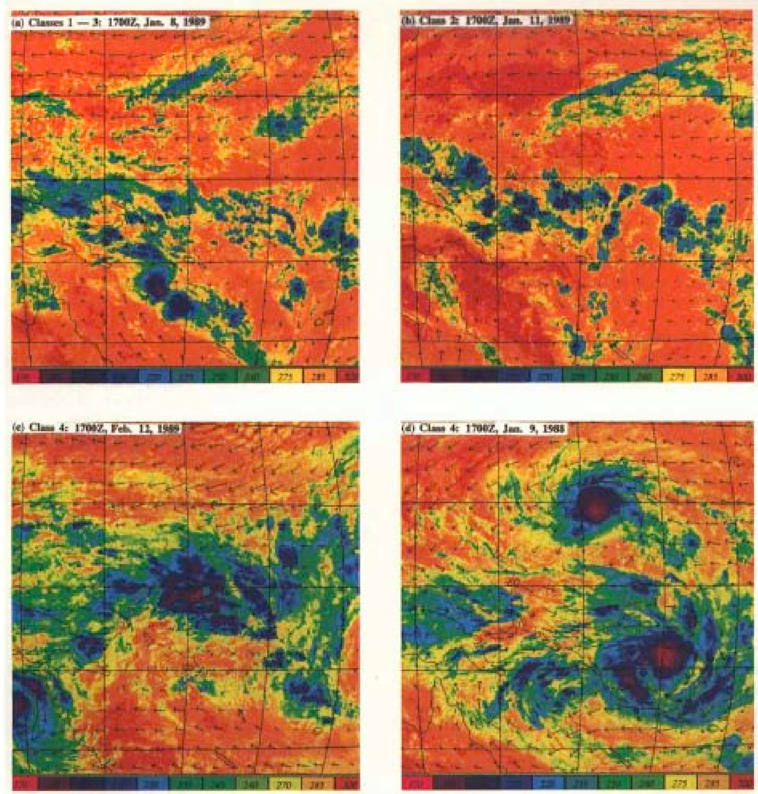

FIG. 9. Four distributions of typical convection types encountered in the western Pacific Ocean. The diagrams show distributions of effective blackbody radiation temperatures relative to the color codes at the base of each panel. The arrows indicate 850-mb wind fields from ECMWF model data. The classes of convection will be referred to later. Figures compile by R. A. Houze, Jr. and Shuyi Chen. (a) Generally undisturbed conditions in a light wind regime. Near the equator, there are a number of small convective elements. The line of convection extending from the equator to the southeast is associated with the Solomon Islands. (b) Relatively disturbed period convective elements of order 100-km diameter between the equator and 10°S. (c) Disturbed period typified by mesoscale and large-scale convective structures along the equator. (d) Synoptic-scale disturbances where mesoscale structures have developed into typhoon intensity. The typhoon pair propagated westward and poleward in their respective hemispheres. Note the strong westerlies over the equator between the cyclone pair, the winds were considerably stregthened by the cyclonic development.

Webster and Lukas, *BAMS* 1992 (TOGA COARE)

The really strong precipitation and heating often comes from convective cloud systems that are large in horizontal extent, and have two distinct regions

Trailing stratiform anvil

Leading line, or convective region

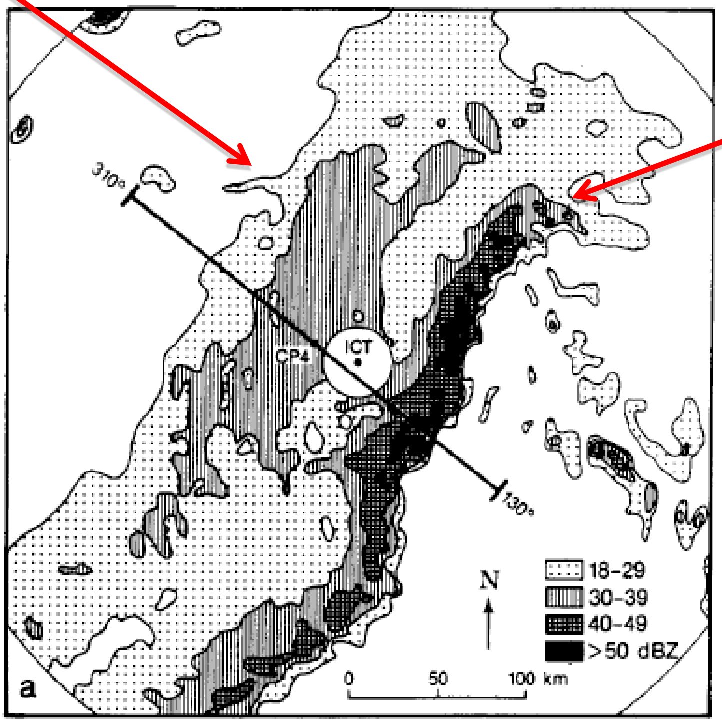

Radar reflectivity, Kansas squall line, “PRE-STORM Experiment (Smull and Houze 1987)

Along-line cross-sections for same storm

“bright band”

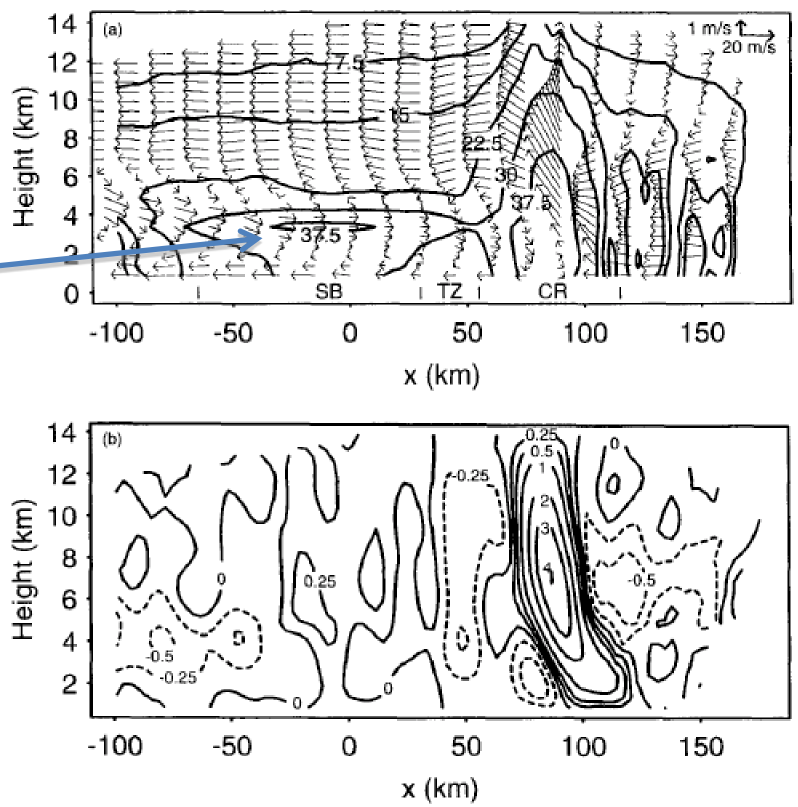

Radar reflectivity (dBz)

Vertical velocity (m/s)

(Smull and Houze 1987)

Bright band in radar image from DYNAMO, Maldives, November 27 2011

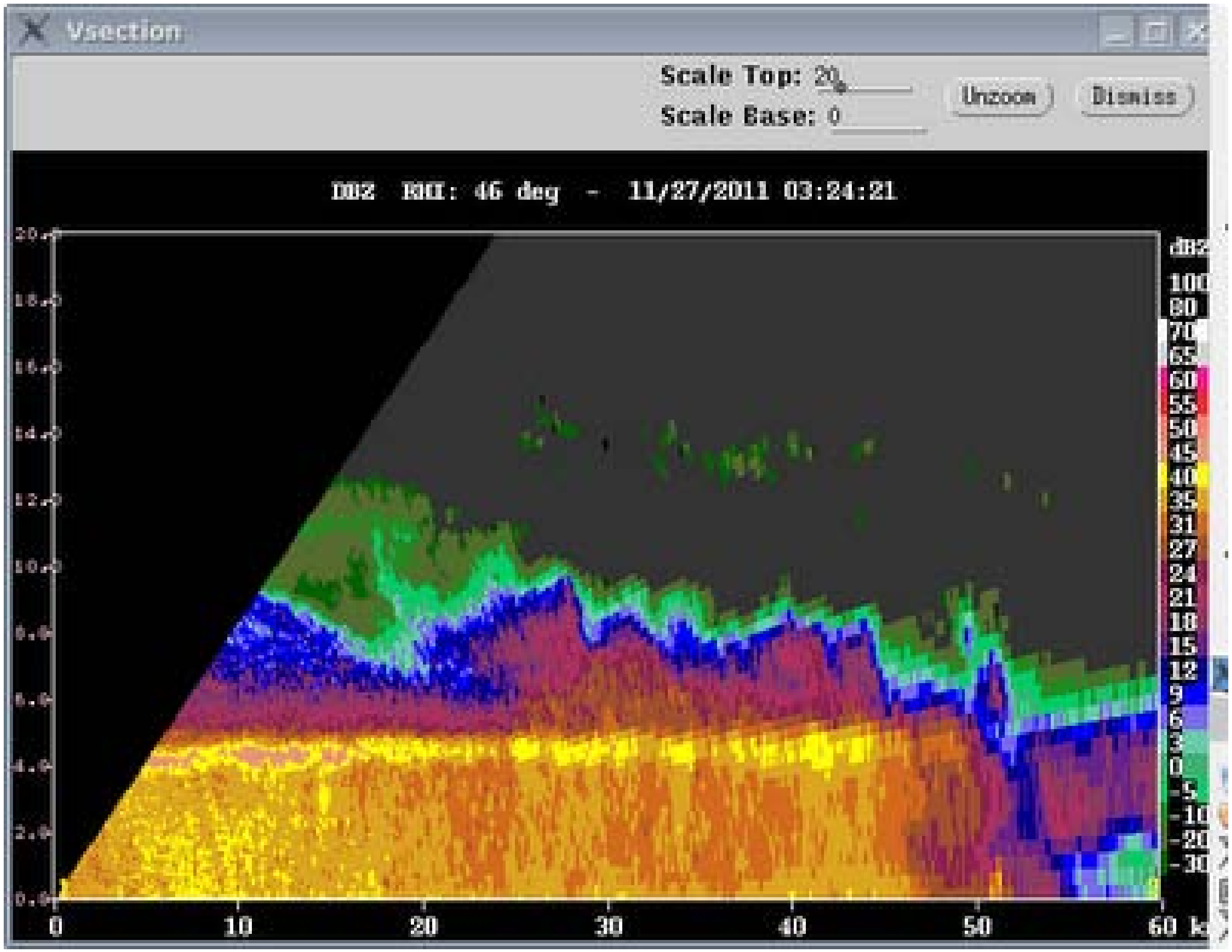

In convective region updraft vertical velocities > terminal velocity of hydrometeors;
In stratiform region converse is true.

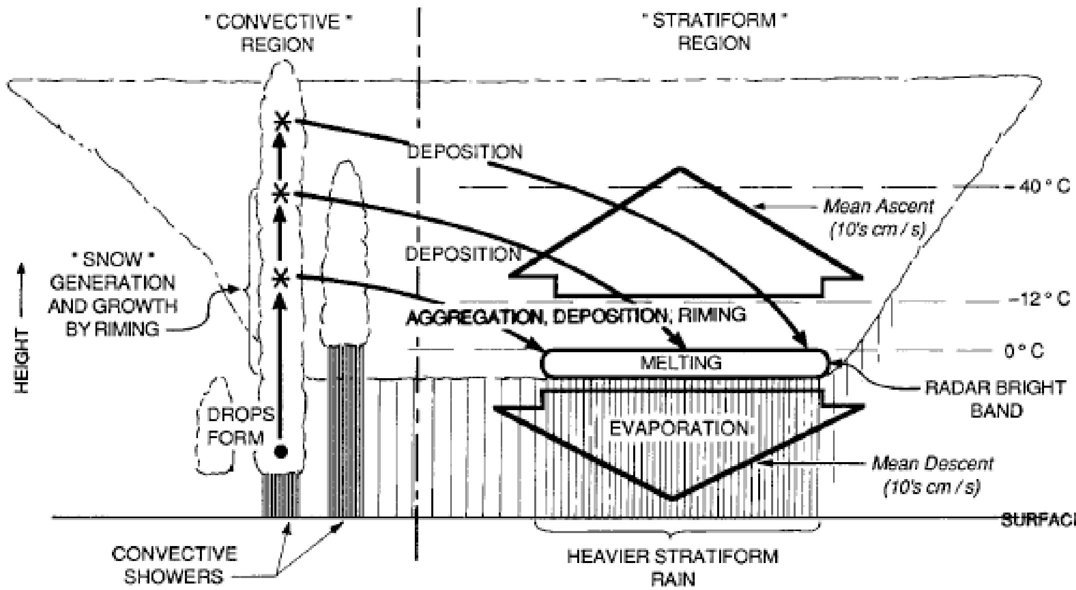

Figure 2. Schematic diagram of the precipitation mechanisms in a tropical cloud system. Solid arrows indicate particle trajectories (adapted from Houze 1989).

Houze, R. A., Jr, 1989: Quart. J. Roy. Met. Soc., 115, 425-461

Next few slides on mesoscale convective systems from Sandra Yuter, NC State

Particle growth mechanisms

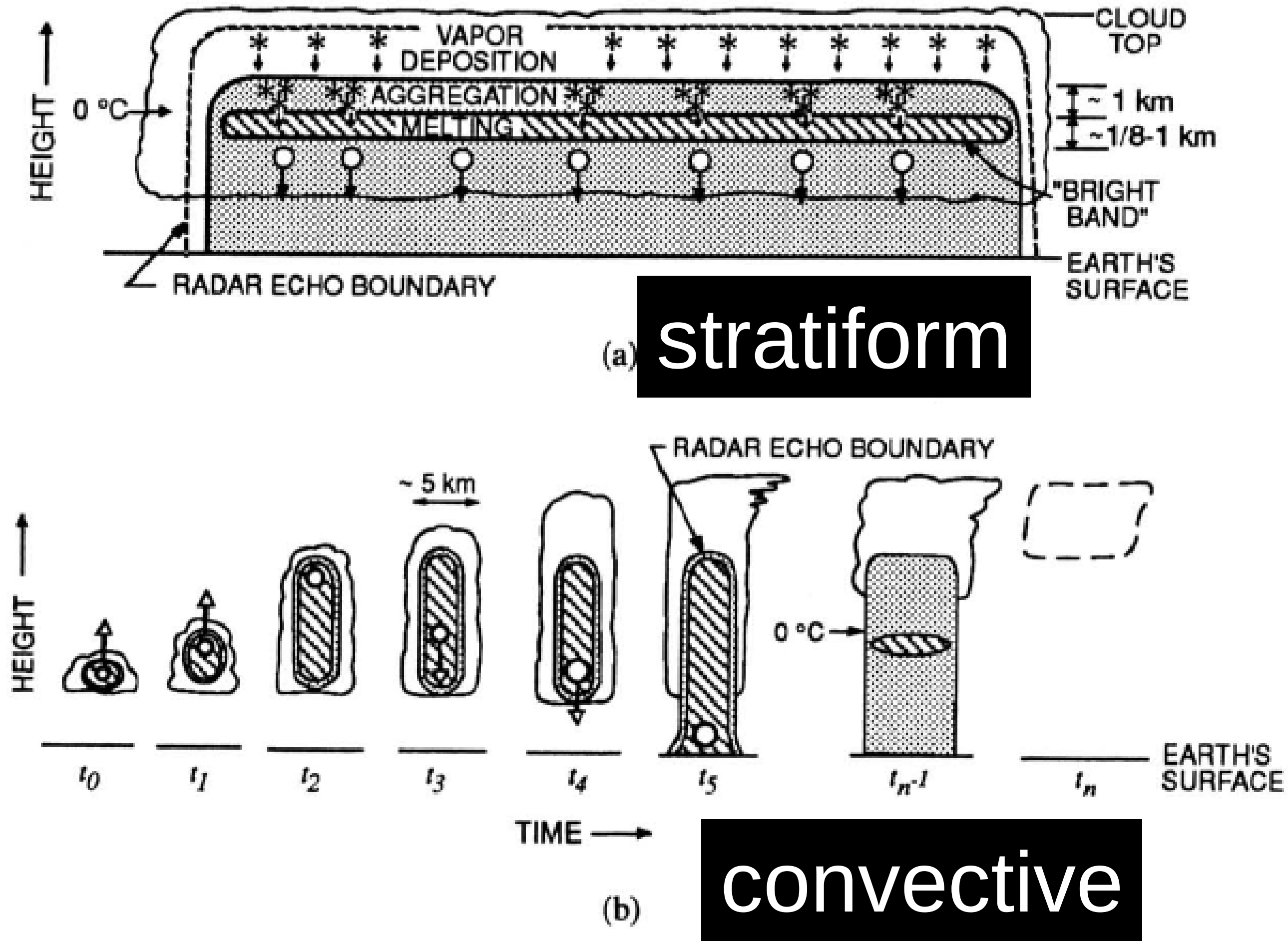

Accretional growth = riming and collision/coalescence

Shading shows higher intensities of radar echo, with hatching indicating the strongest echo. In (b) cloud is shown at a succession of times t0, ,,,,tn. Growing precipitation particle is carried upward by strong updrafts until t2 and then falls relative to the ground, reaching the surface just after t5. After t5 the cloud may die or continue for a considerable time in a steady state before dissipation sets in at tn-1 and tn,. The dashed boundary indicates evaporating cloud.

Particle growth mechanisms

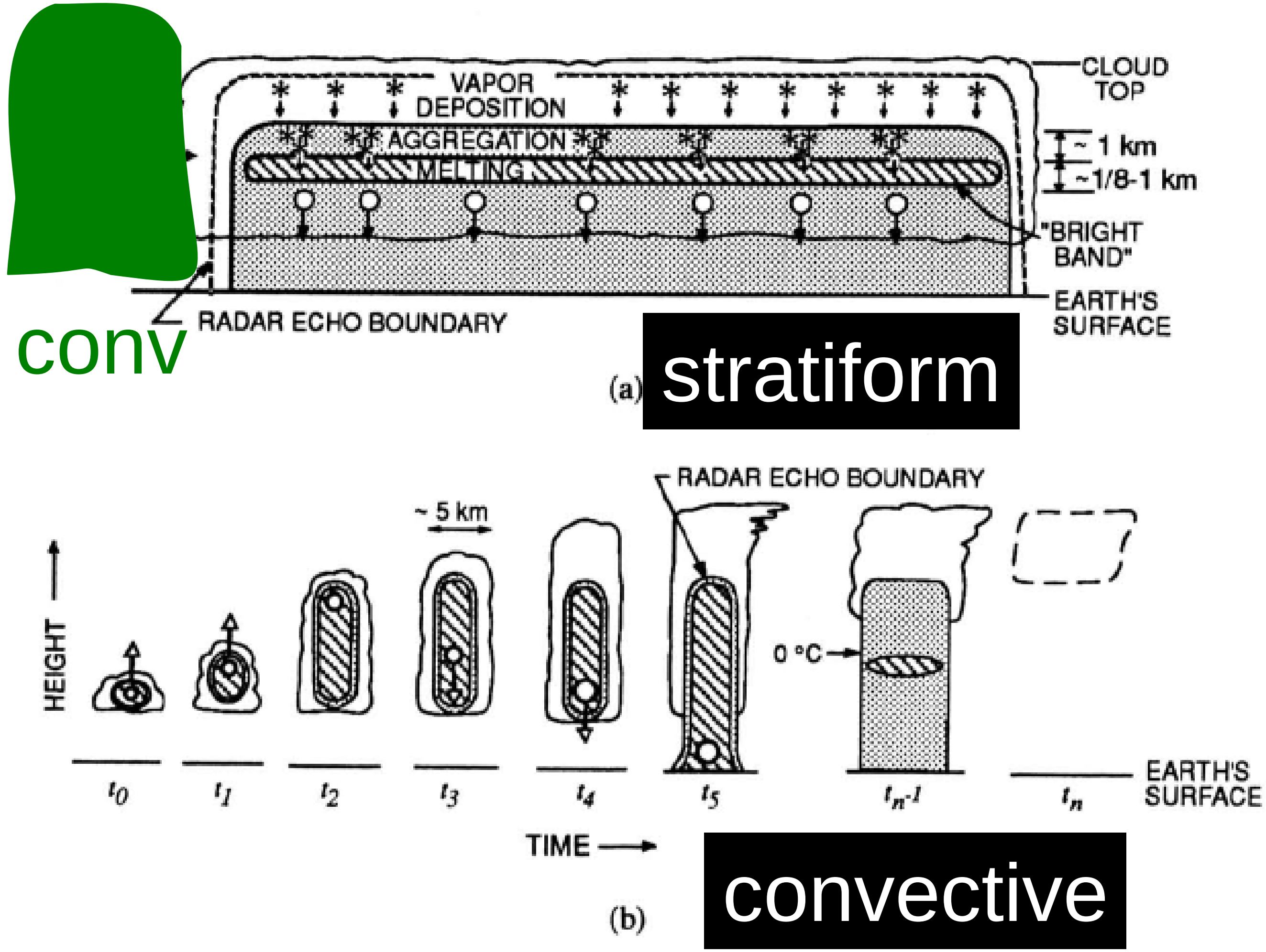

Accretional growth = riming and collision/coalescence

Shading shows higher intensities of radar echo, with hatching indicating the strongest echo. In (b) cloud is shown at a succession of times t0, ,,,,tn. Growing precipitation particle is carried upward by strong updrafts until t2 and then falls relative to the ground, reaching the surface just after t5. After t5 the cloud may die or continue for a considerable time in a steady state before dissipation sets in at tn-1 and tn,. The dashed boundary indicates evaporating cloud.

Particle growth mechanisms

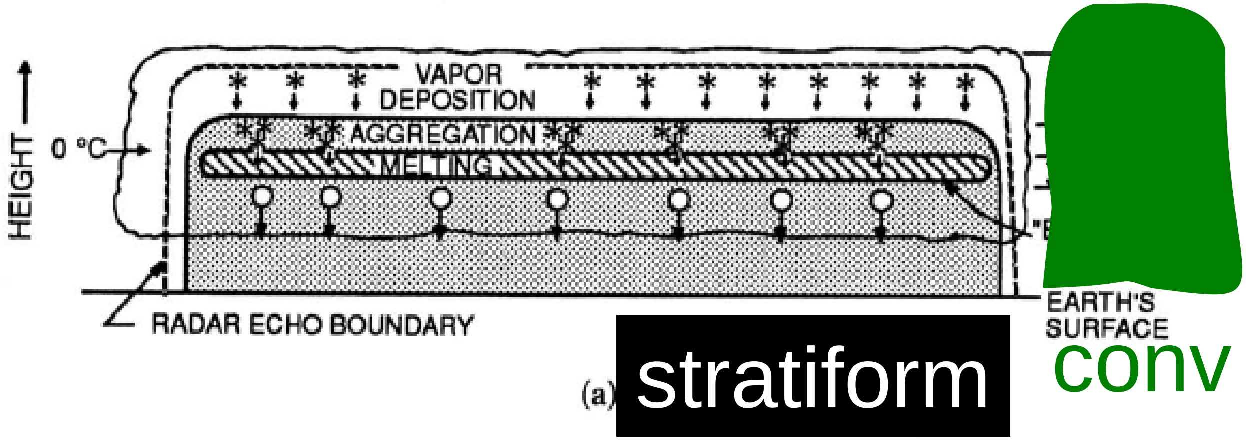

(a)

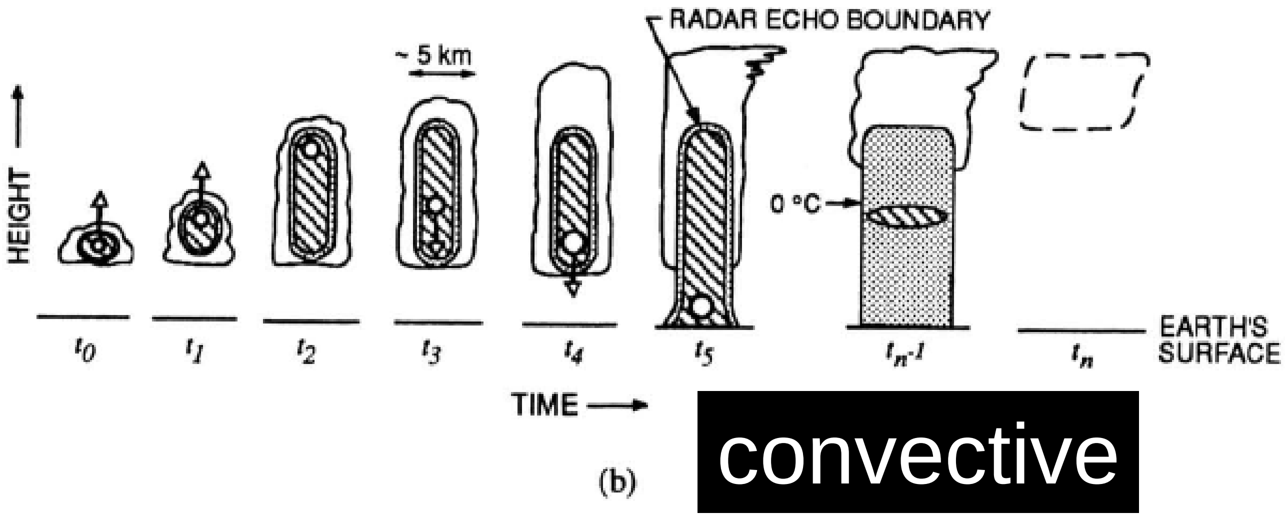

(b)

Accretional growth = riming and collision/coalescence

Shading shows higher intensities of radar echo, with hatching indicating the strongest echo. In (b) cloud is shown at a succession of times t0, ,,,,tn. Growing precipitation particle is carried upward by strong updrafts until t2 and then falls relative to the ground, reaching the surface just after t5. After t5 the cloud may die or continue for a considerable time in a steady state before dissipation sets in at tn-1 and tn,. The dashed boundary indicates evaporating cloud.

Mesoscale convective system = a cumulonimbus cloud system that produces a contiguous area ~100 km or more in at least one direction

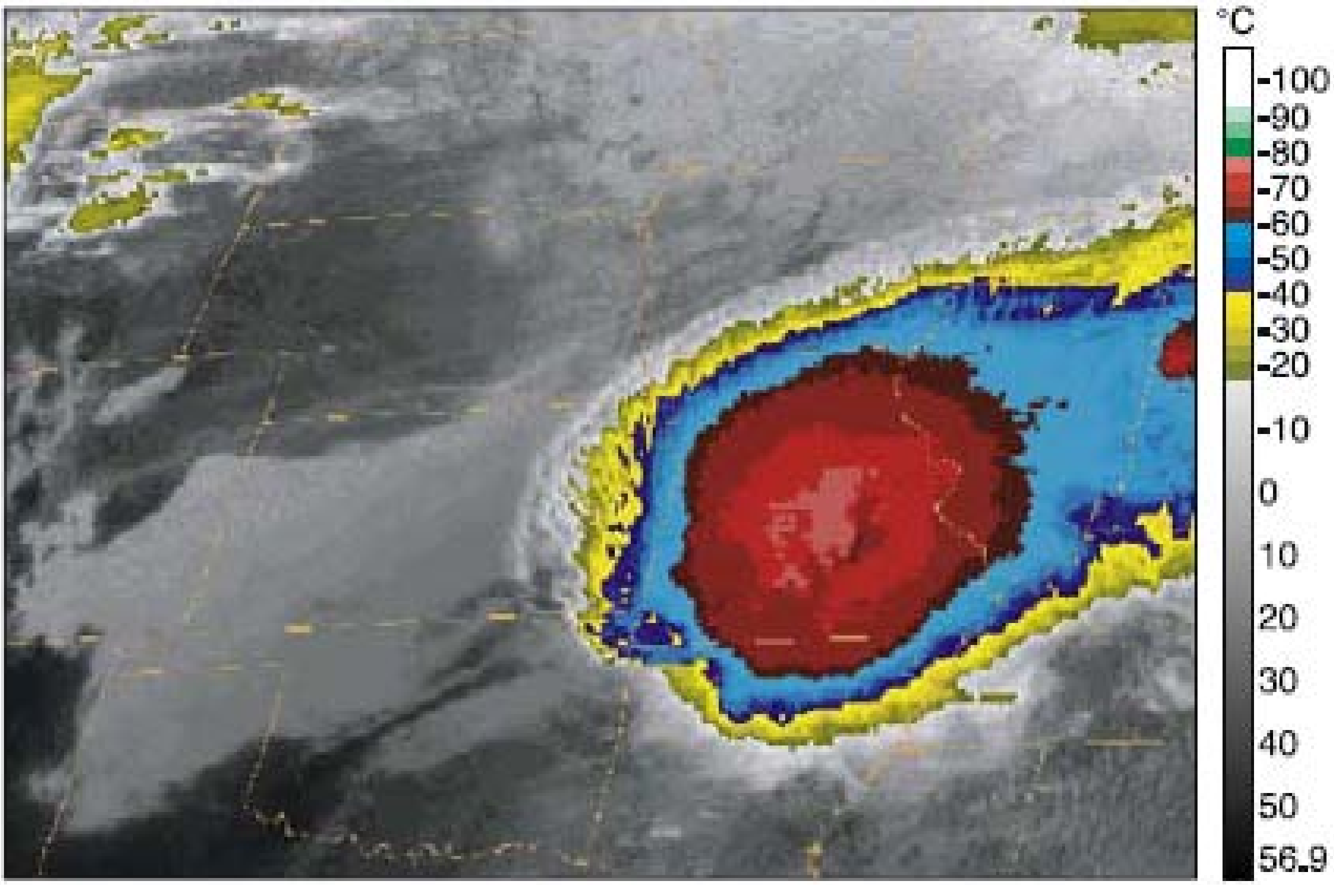

IR image

Slide by Sandra Yuter

MCS

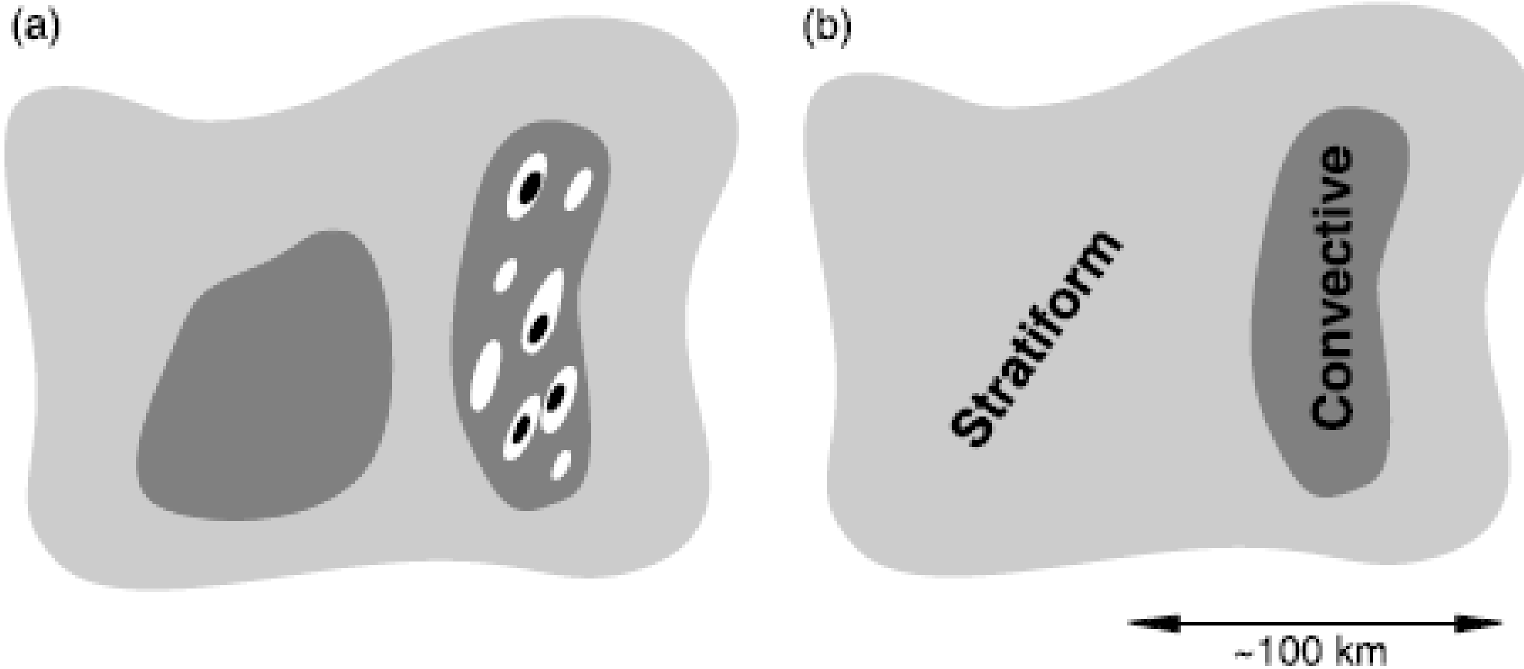

Idealized horizontal map of radar reflectivity

Convective and stratiform precipitation regions

Slide by Sandra Yuter

Definitions of Tropical Precipitation Types

from Houze (1997) and applied in Steiner et al. (1995) and TRMM algorithms (1997)

1) Convective
Young, vigorous convection
Cellular, vertically-oriented reflectivity maxima
Dominant accretional growth of precipitation
“Convective” latent heating profile

Slide by Sandra Yuter

Definitions of Tropical Precipitation Types

from Houze (1997) and applied in Steiner et al. (1995) and TRMM algorithms (1997)

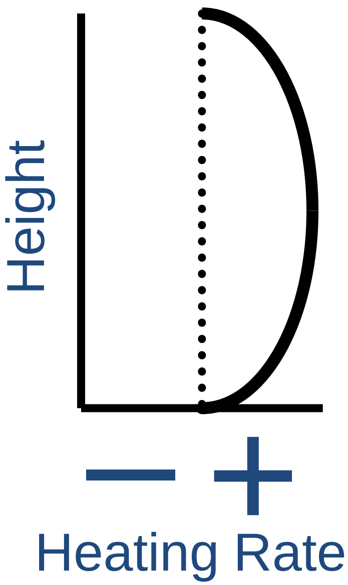

1) Convective
Young, vigorous convection
Cellular, vertically-oriented reflectivity maxima
Dominant accretional growth of precipitation
“Convective” latent heating profile

Slide by Sandra Yuter

Definitions of Tropical Precipitation Types

from Houze (1997) and applied in Steiner et al. (1995) and TRMM algorithms (1997)

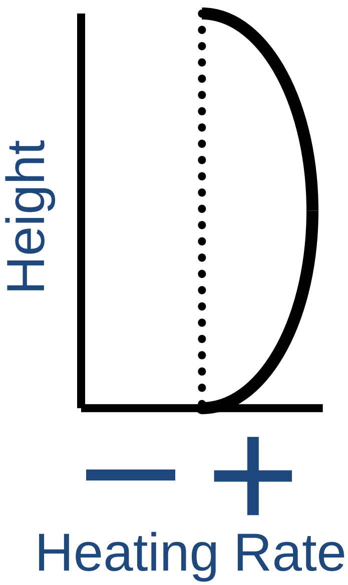

1) Convective	2) **Stratiform**
Young, vigorous convection	Old convection
Cellular, vertically-oriented reflectivity maxima	Relatively homogenous in the horizontal, layered reflectivity structure
Dominant accretional growth of precipitation	Dominant vapor deposition growth of precipitation
"Convective" latent heating profile	"Stratiform" latent heating profile

Slide by Sandra Yuter

Definitions of Tropical Precipitation Types

from Houze (1997) and applied in Steiner et al. (1995) and TRMM algorithms (1997)

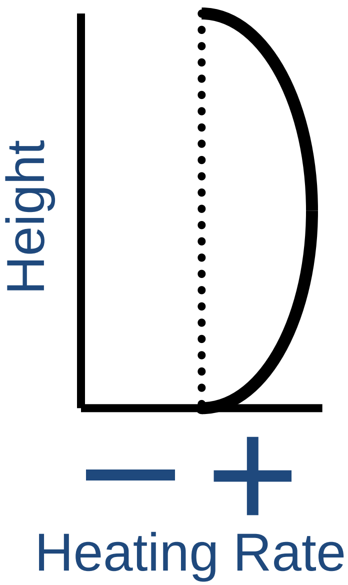

1) Convective	2) **Stratiform**
Young, vigorous convection	Old convection
Cellular, vertically-oriented reflectivity maxima	Relatively homogenous in the horizontal, layered reflectivity structure
Dominant accretional growth of precipitation	Dominant vapor deposition growth of precipitation
"Convective" latent heating profile	"Stratiform" latent heating profile

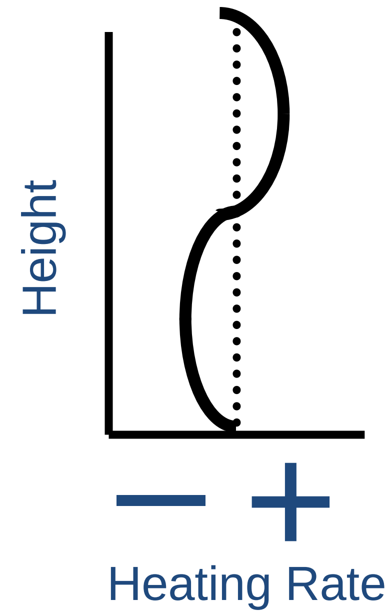

Slide by Sandra Yuter

Definitions of Tropical Precipitation Types

from Houze (1997) and applied in Steiner et al. (1995) and TRMM algorithms (1997)

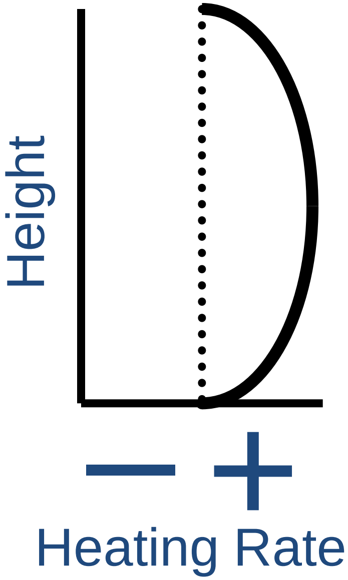

1) Convective	2) **Stratiform**
Young, vigorous convection	Old convection
Cellular, vertically-oriented reflectivity maxima	Relatively homogenous in the horizontal, layered reflectivity structure
Dominant accretional growth of precipitation	Dominant vapor deposition growth of precipitation
"Convective" latent heating profile	"Stratiform" latent heating profile

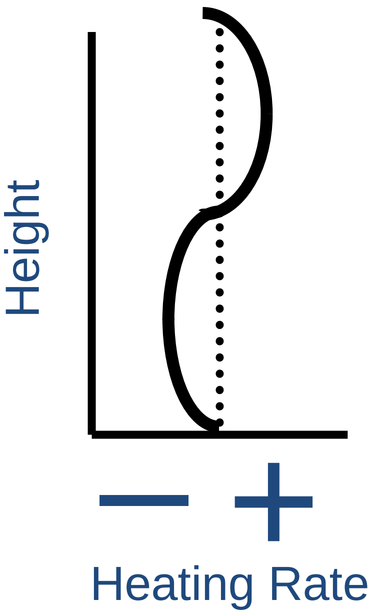

Isolated weak echoes could be either in the initial stages of a developing cell or final stages of mature cell

Slide by Sandra Yuter

Idealized Mesoscale Convective System Storm Structure

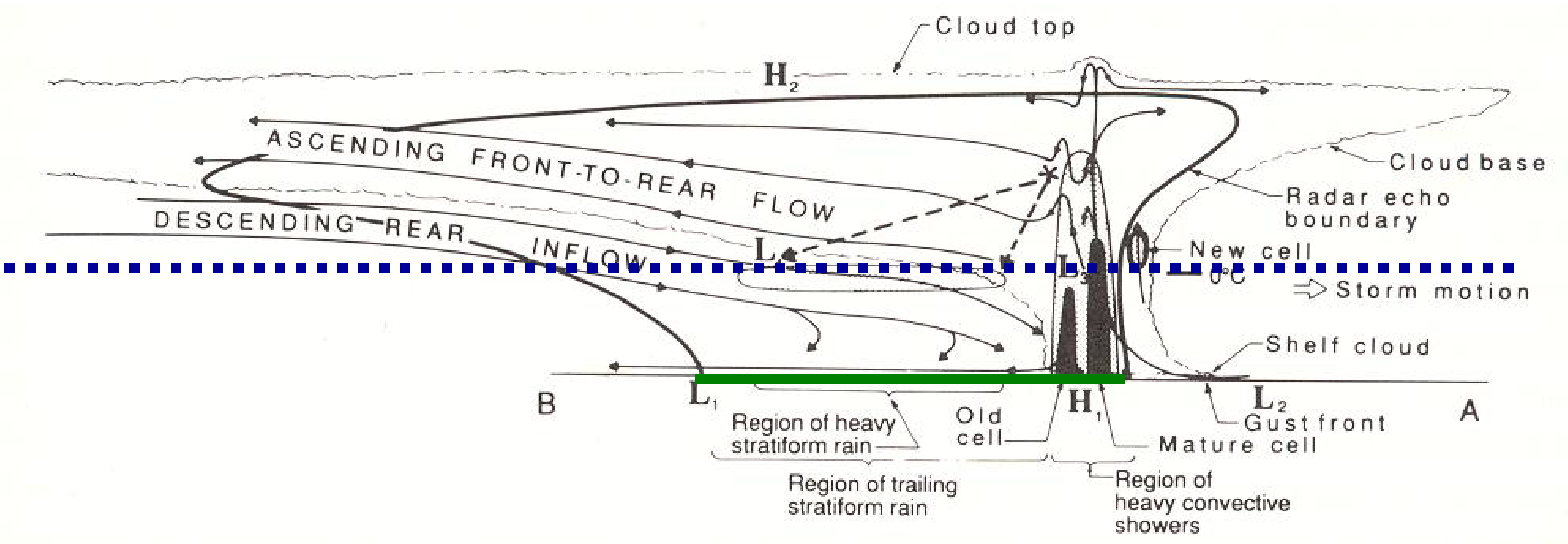

Houze et al. 1989

Slide by Sandra Yuter

Idealized Mesoscale Convective System Storm Structure

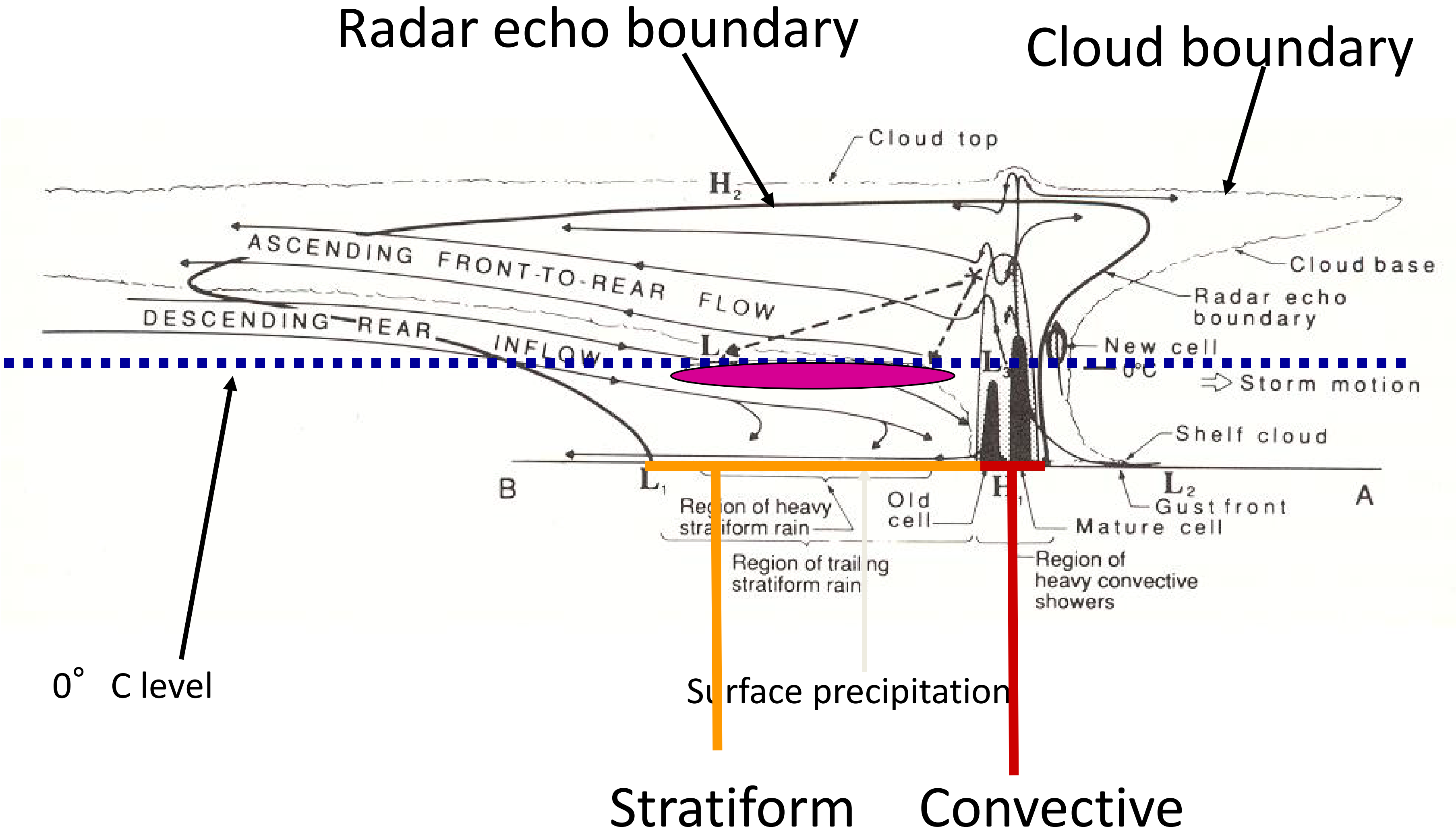

Houze et al. 1989

Slide by Sandra Yuter

convective & stratiform regions have distinctly different vertical structures for the apparent convective heating, though what we observe on large scales is the combination

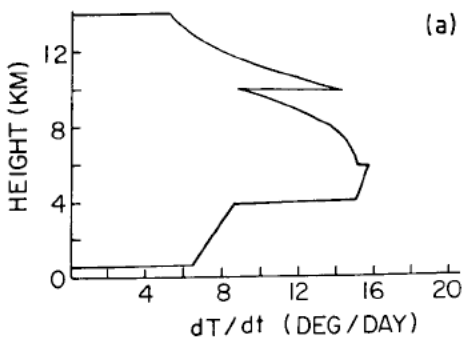

convective

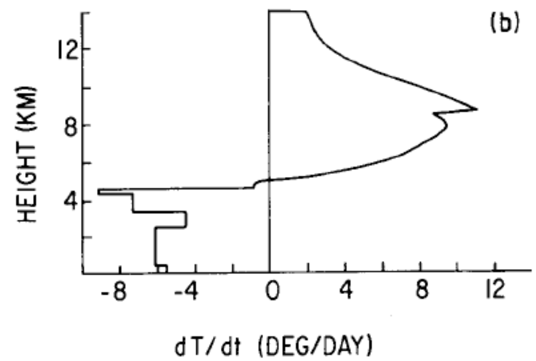

stratiform

Houze 1989

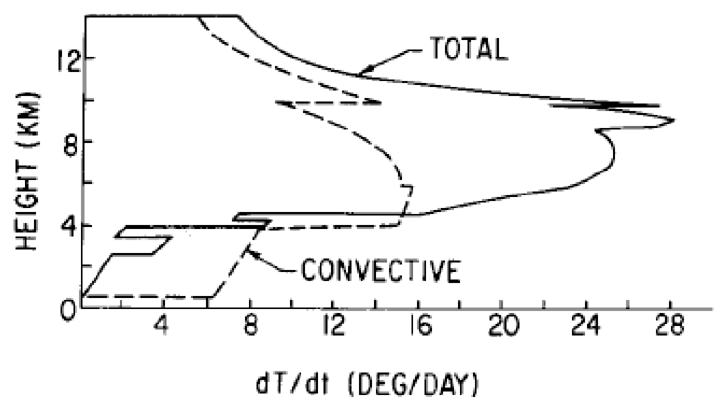

Deep convection over land has a much stronger diurnal cycle and can attain greater intensity

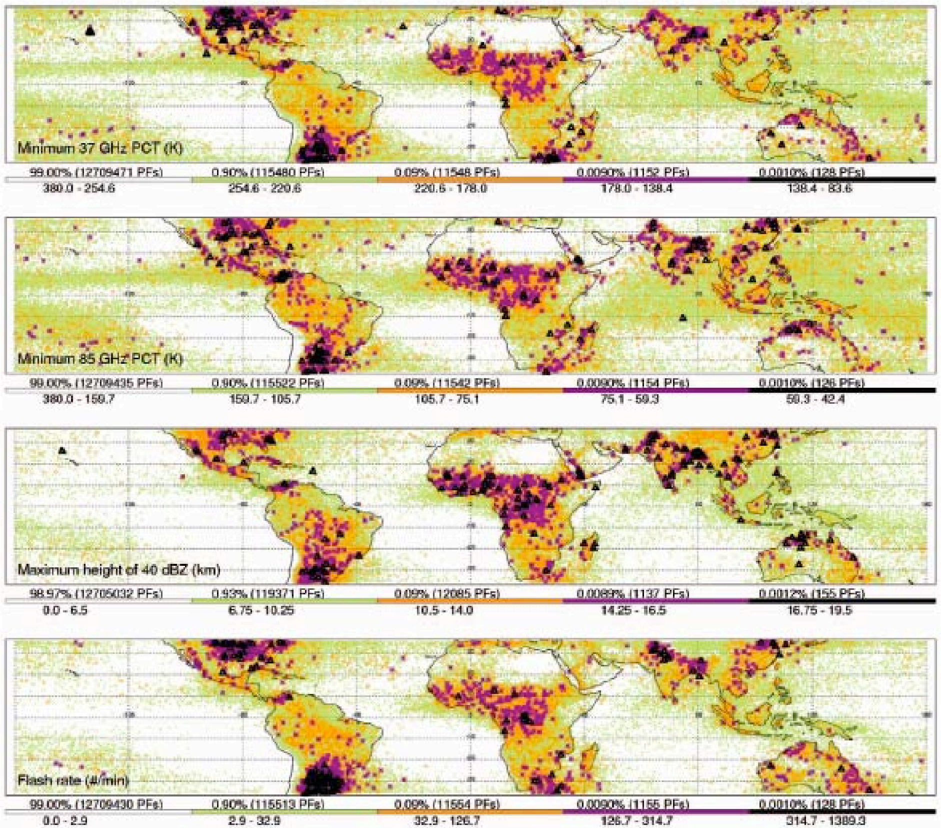

FIG. 3. Locations of intense convective events using the color code matching their rarity. The parameter limits for each category are indicated above each color bar. For example, of the 12.8 million PFs, only about 0.001% (128) have more than 314.7 lightning flashes per minute. The exact percentages for the break points are slightly different from the 40-dBZ echo-top figure because radar data are reported in discrete increments of 250 m.

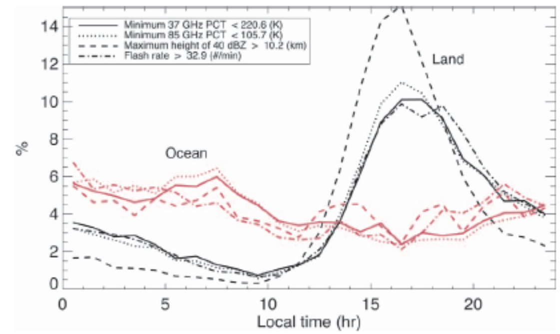

FIG. 5. Diurnal cycle of the three most extreme categories (top 0.1%; Figs. 2 and 3) for each parameter separated by land and ocean PFs. There are not enough extreme events over oceans to use only the top two categories.

Their frequency of occurrence as fn. Of time of day

Frequency of most intense convective systems

Zipser et al. (2006, *BAMS*)

Much more lightning, and deeper convection over land, for same rain amount (Takayabu 2006, Geophys. Res. Lett.)

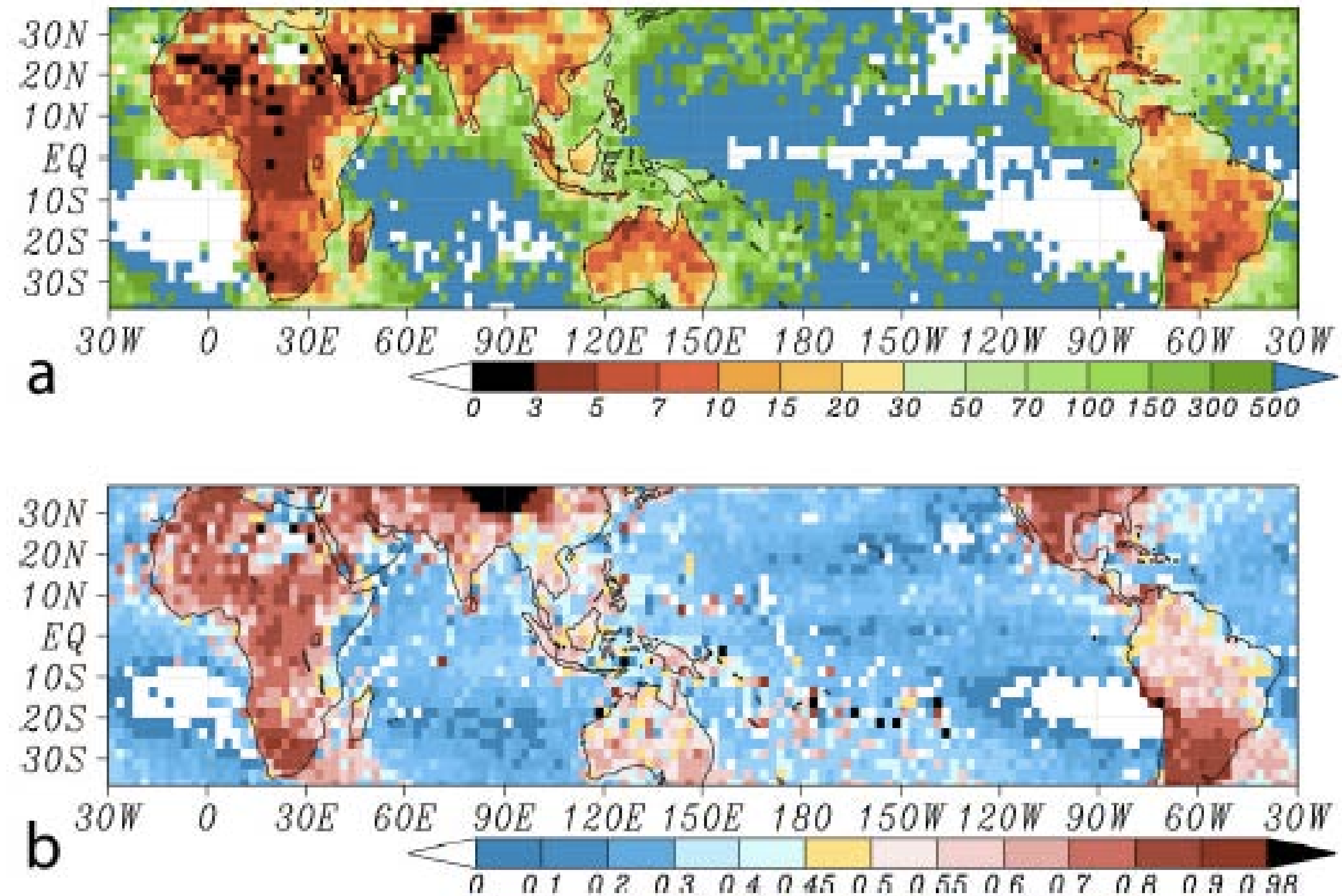

Figure 1. Global distributions of 3-year (March 1998–February 2001) (a) mean Rain-yields per flash and (b) Tall Convective Rain Contribution to surface rain with a threshold of −20degC. Units for the color scales are 10^7 kg fl^{-1} (Figure 1a) and fraction contribution (0–1) (Figure 1b). RPF averages are obtained by dividing the total precipitation amount by the total flash number for the averaging period.

Example of very severe, long-lived squall line:
2012 derecho in USA

http://www.crh.noaa.gov/iwx/?n=june_29_derecho

Strong low-level vertical wind shear is favorable for strong, long-lived squall lines, due to interaction with cold pools (Rotunno, Klemp & Weisman 1988)

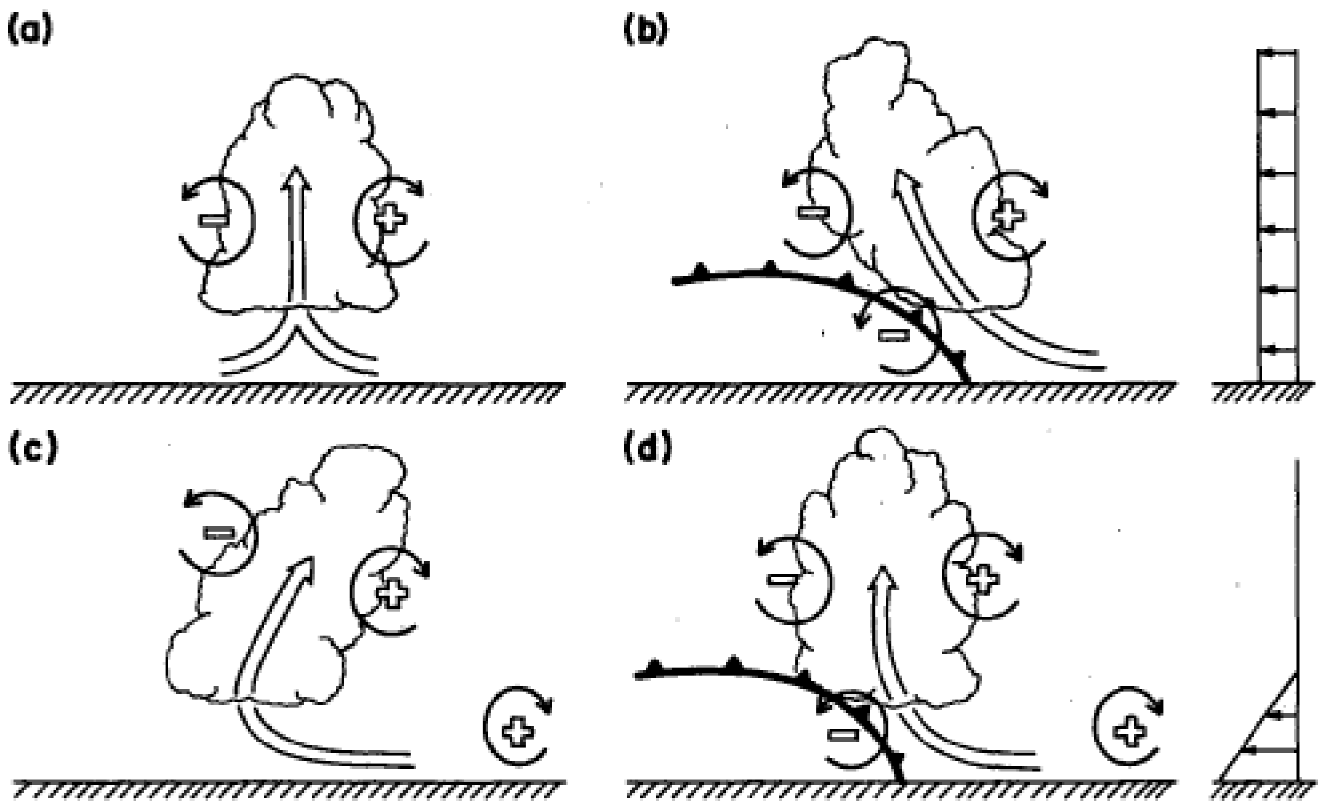

FIG. 18. Schematic diagram showing how a buoyant updraft may be influenced by wind shear and/or a cold pool. (a) With no shear and no cold pool, the axis of the updraft produced by the thermally created, symmetric vorticity distribution is vertical. (b) With a cold pool, the distribution is biased by the negative vorticity of the underlying cold pool and causes the updraft to lean upshear. (c) With shear, the distribution is biased toward positive vorticity and this causes the updraft to lean back over the cold pool. (d) With both a cold pool and shear, the two effects may negate each other, and allow an erect updraft.

Climatology of precipitation and related fields from ERA40 Atlas

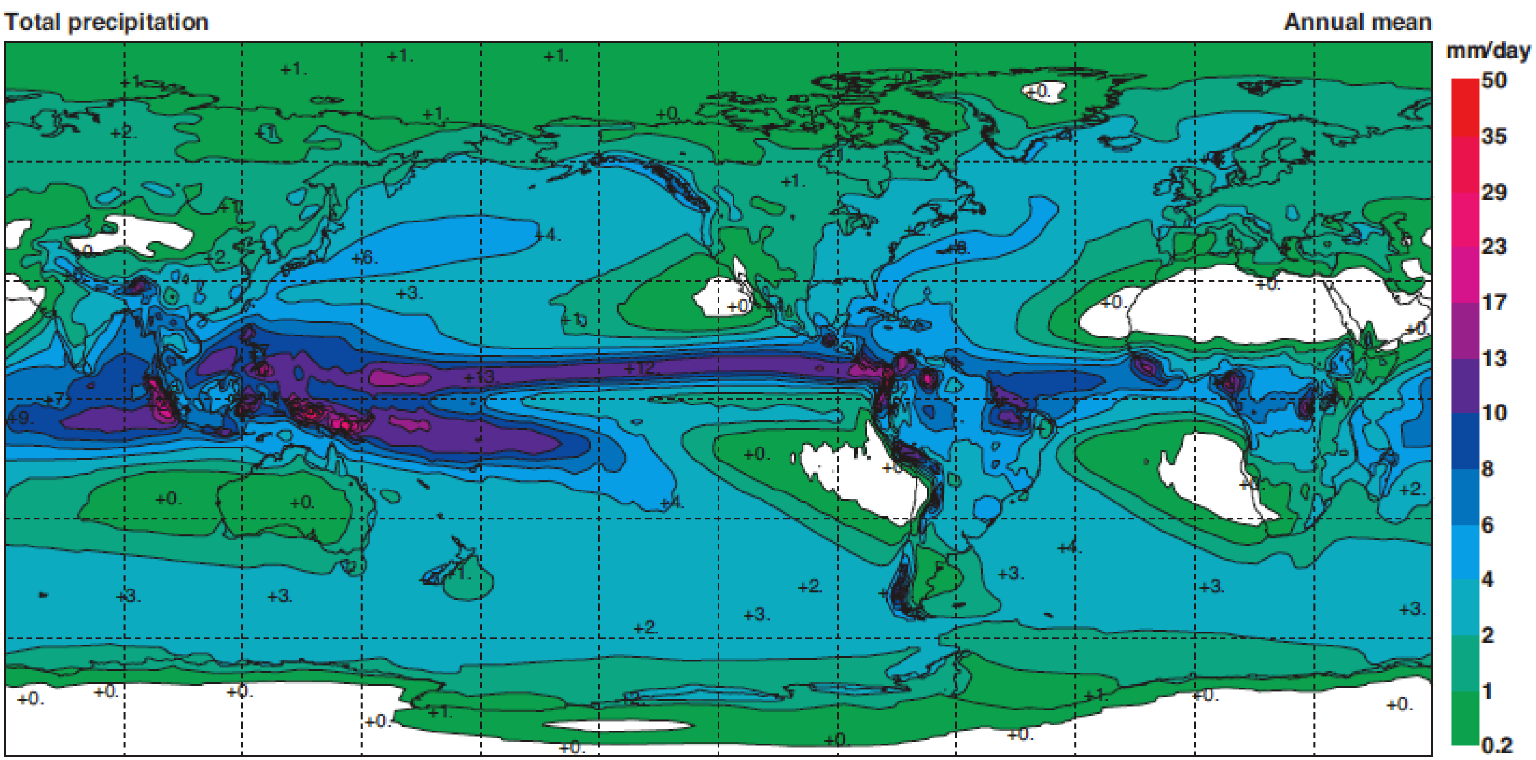
Total precipitation
Annual mean
mm/day
50
35
29
23
17
13
10
8
6
4
2
1
0.2

Precipitation – DJF & JJA

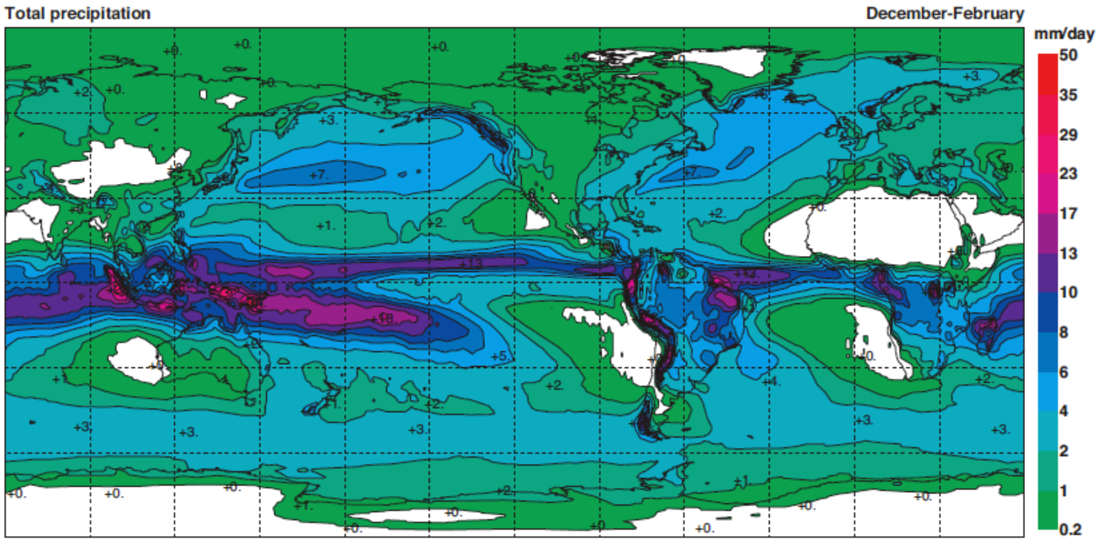

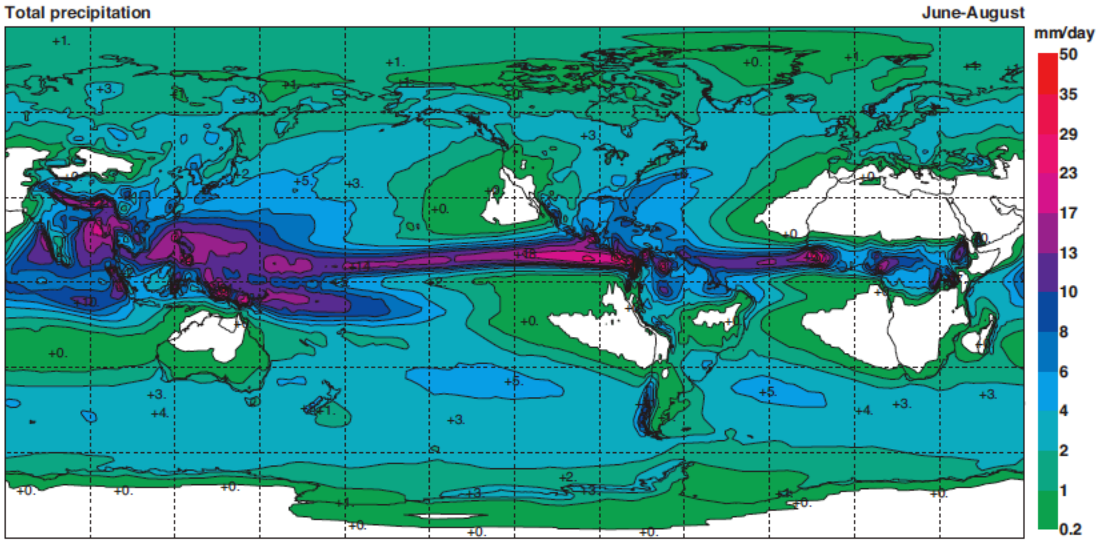

Precipitation – MAM & SON

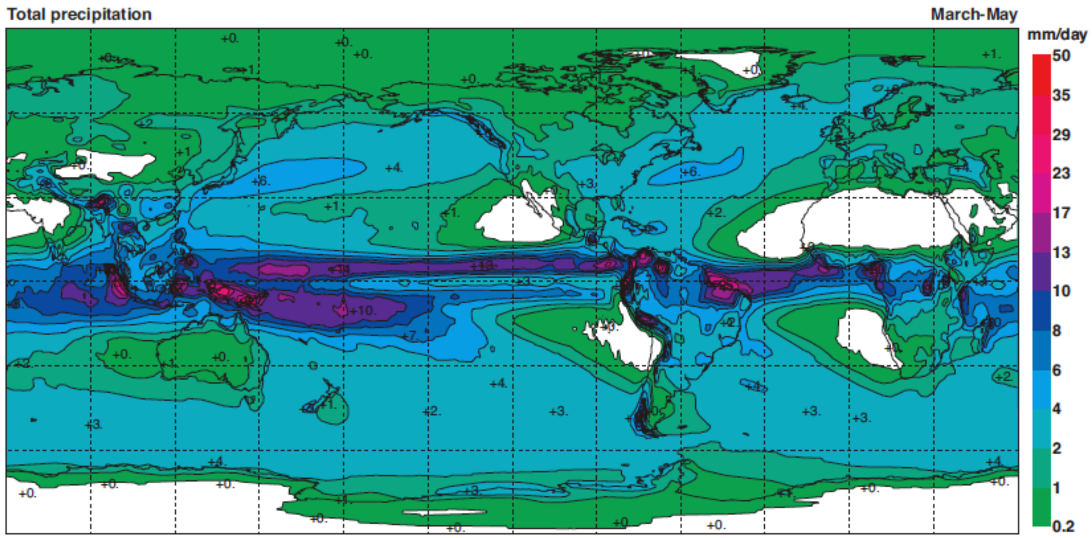

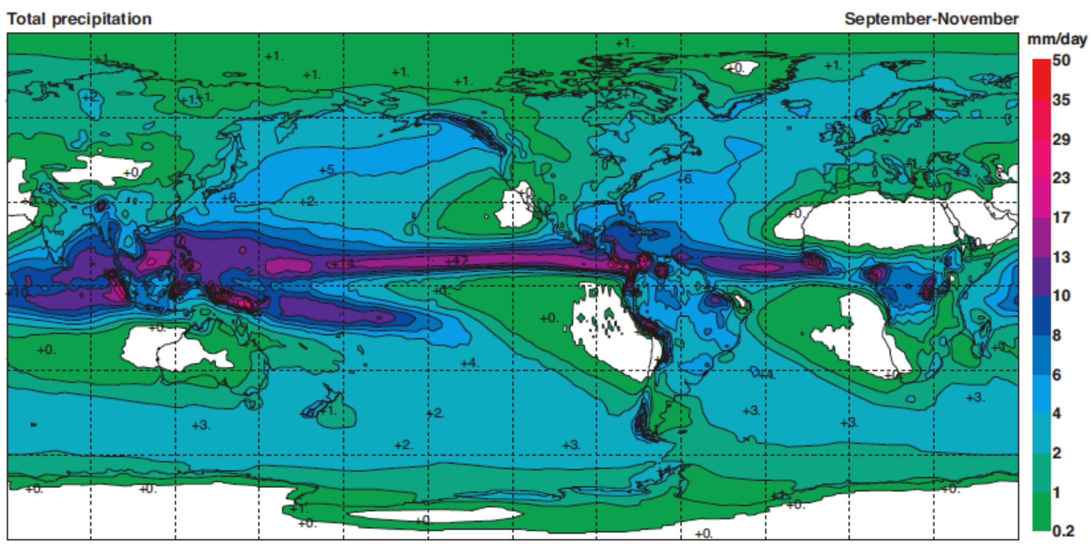

500 hPa omega & Precipitation, annual mean

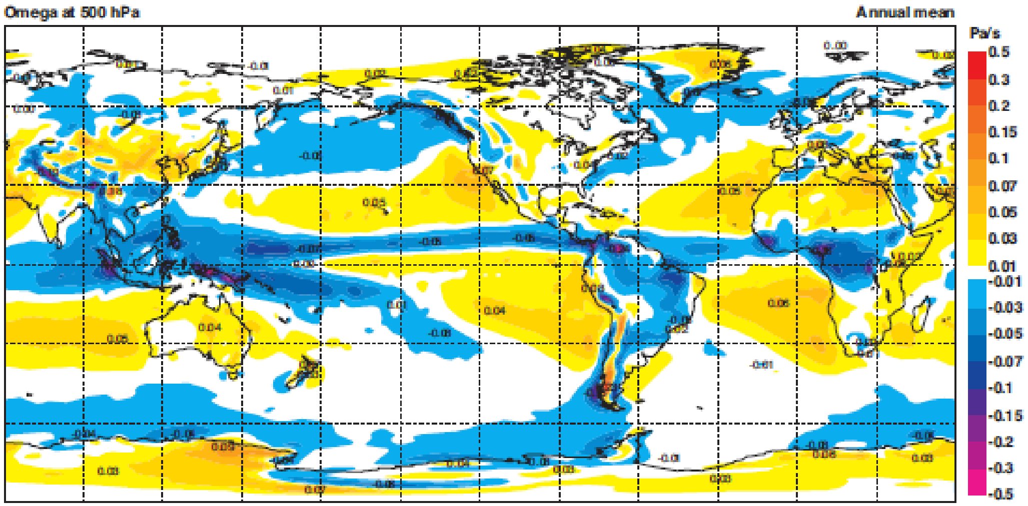

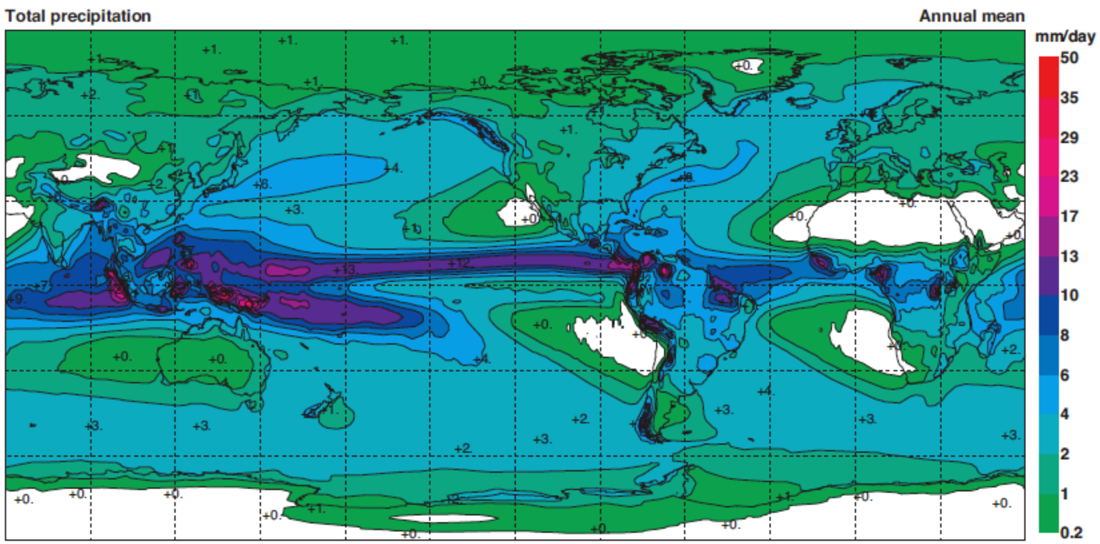

500 hPa omega, DJF & JJA

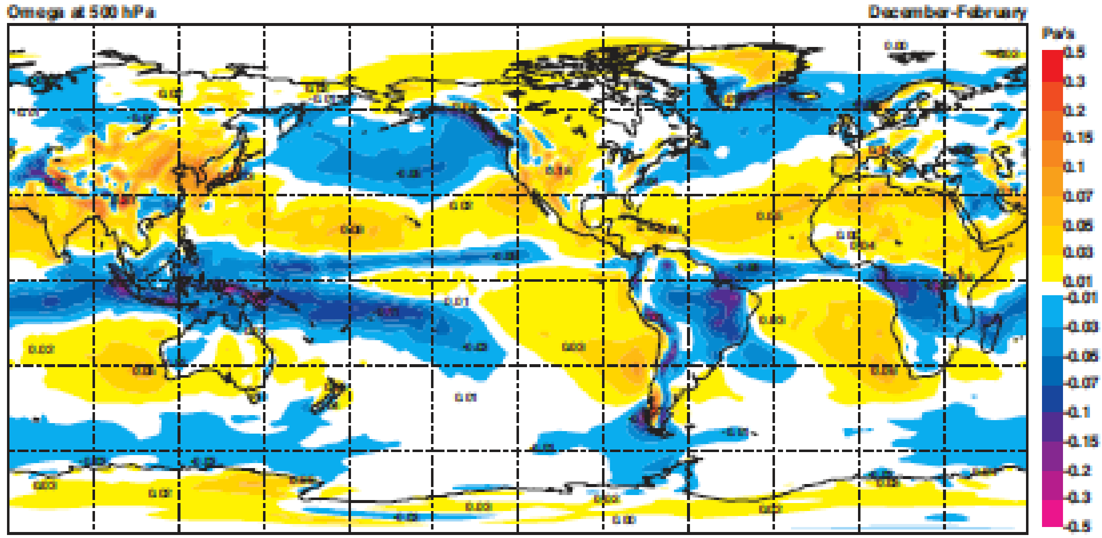

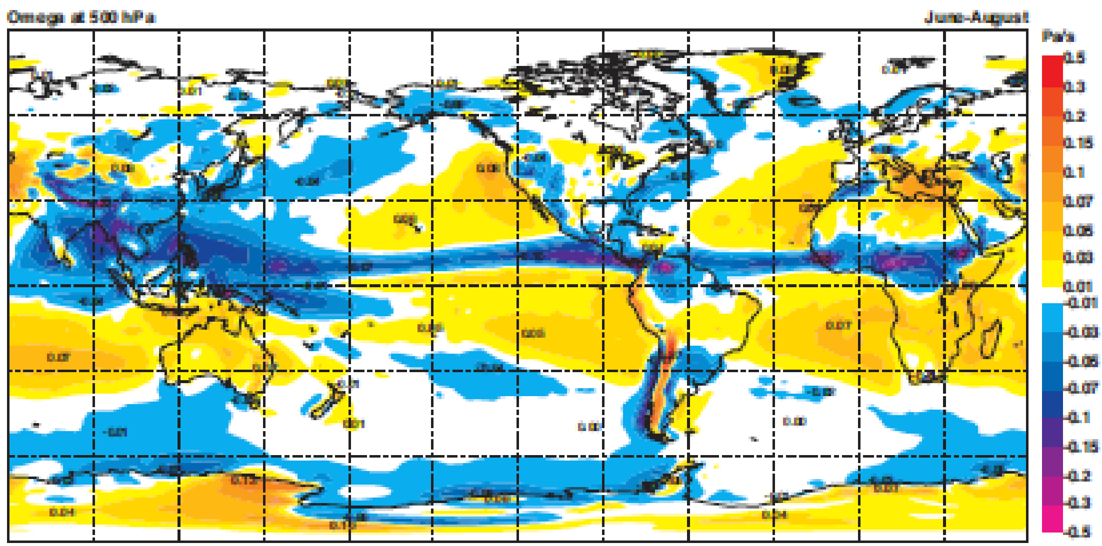

500 hPa omega, MAM & SON

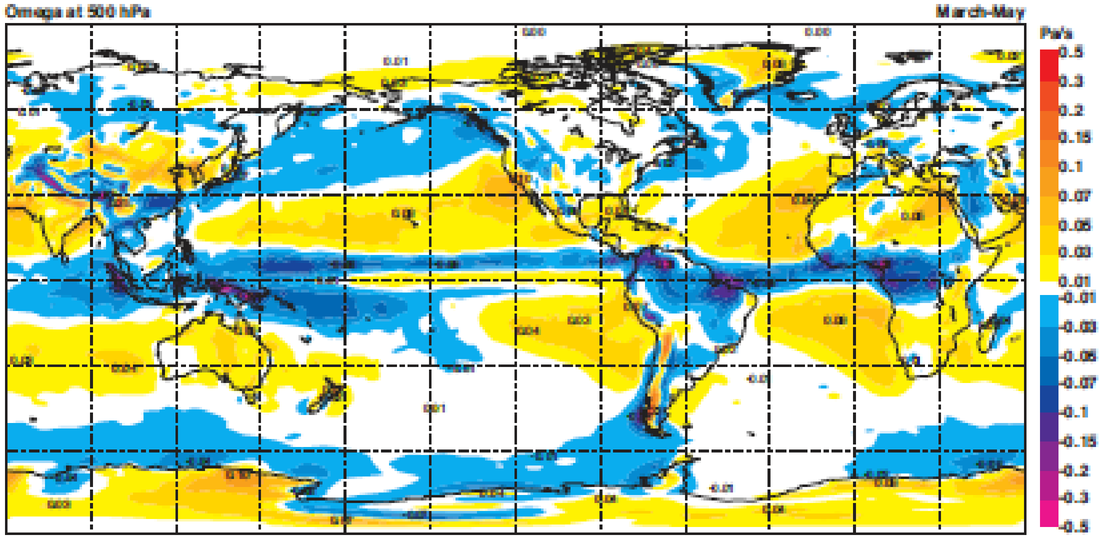

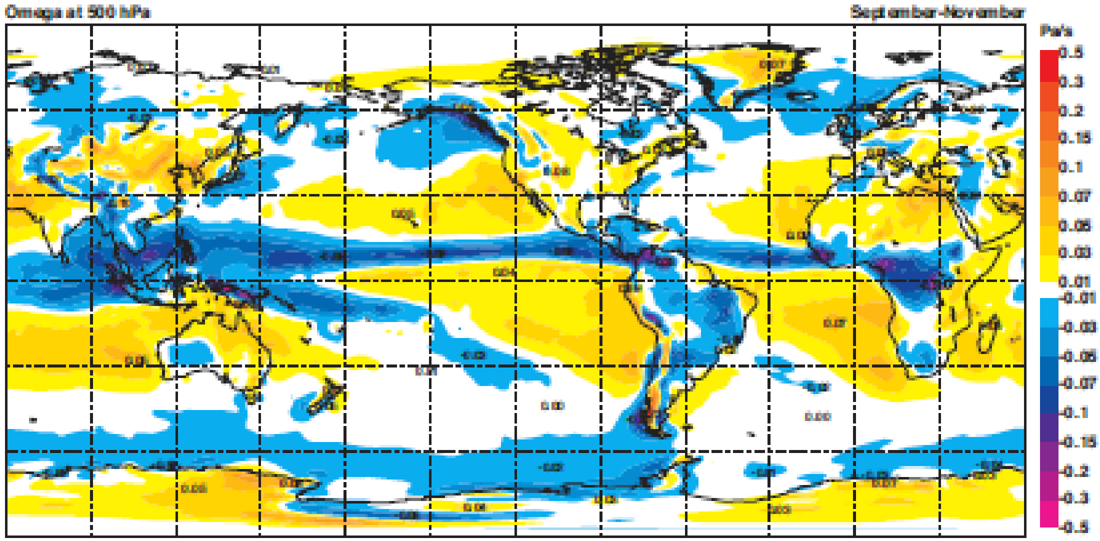

Column-integrated “diabatic heating” and precipitation, annual mean

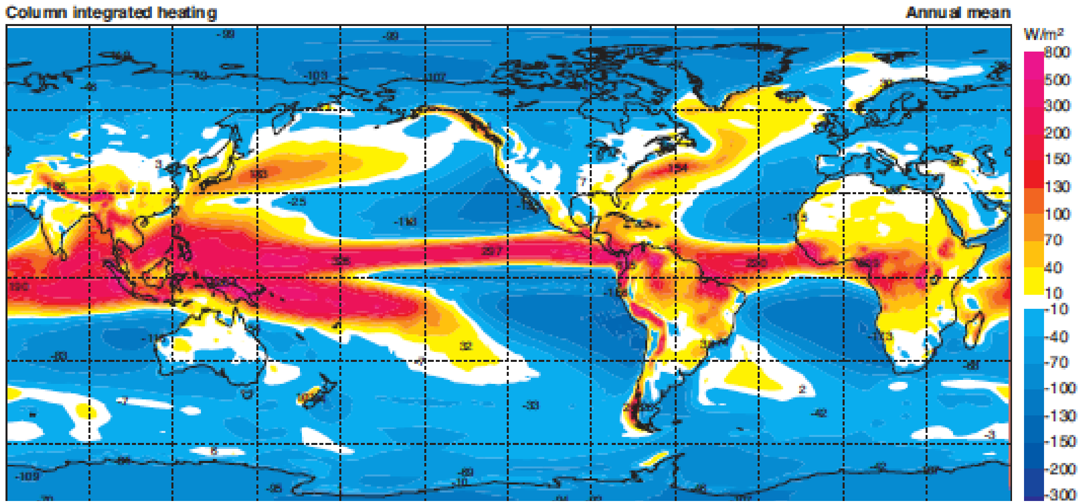

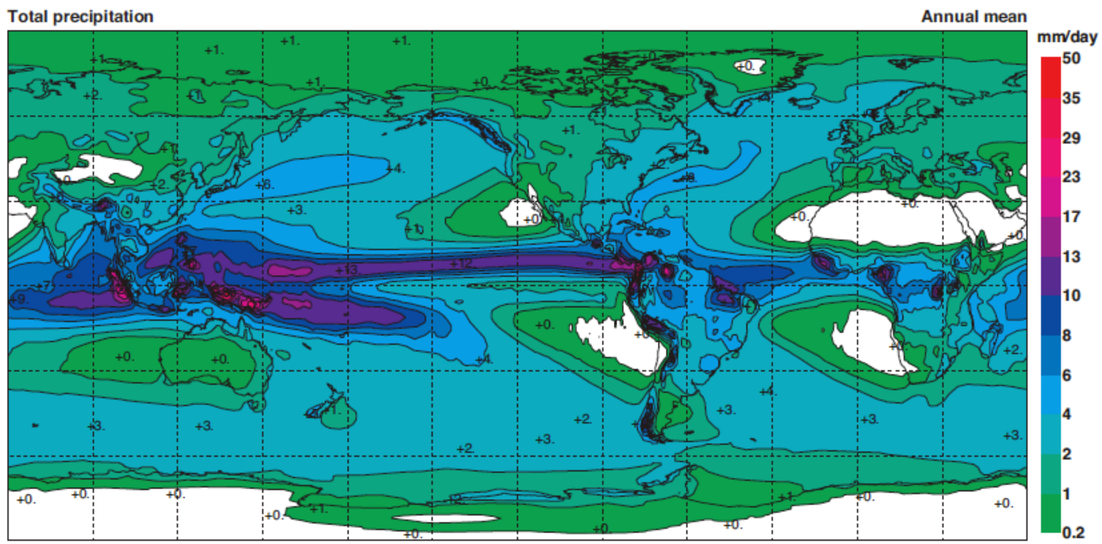

Heating, DJF & JJA

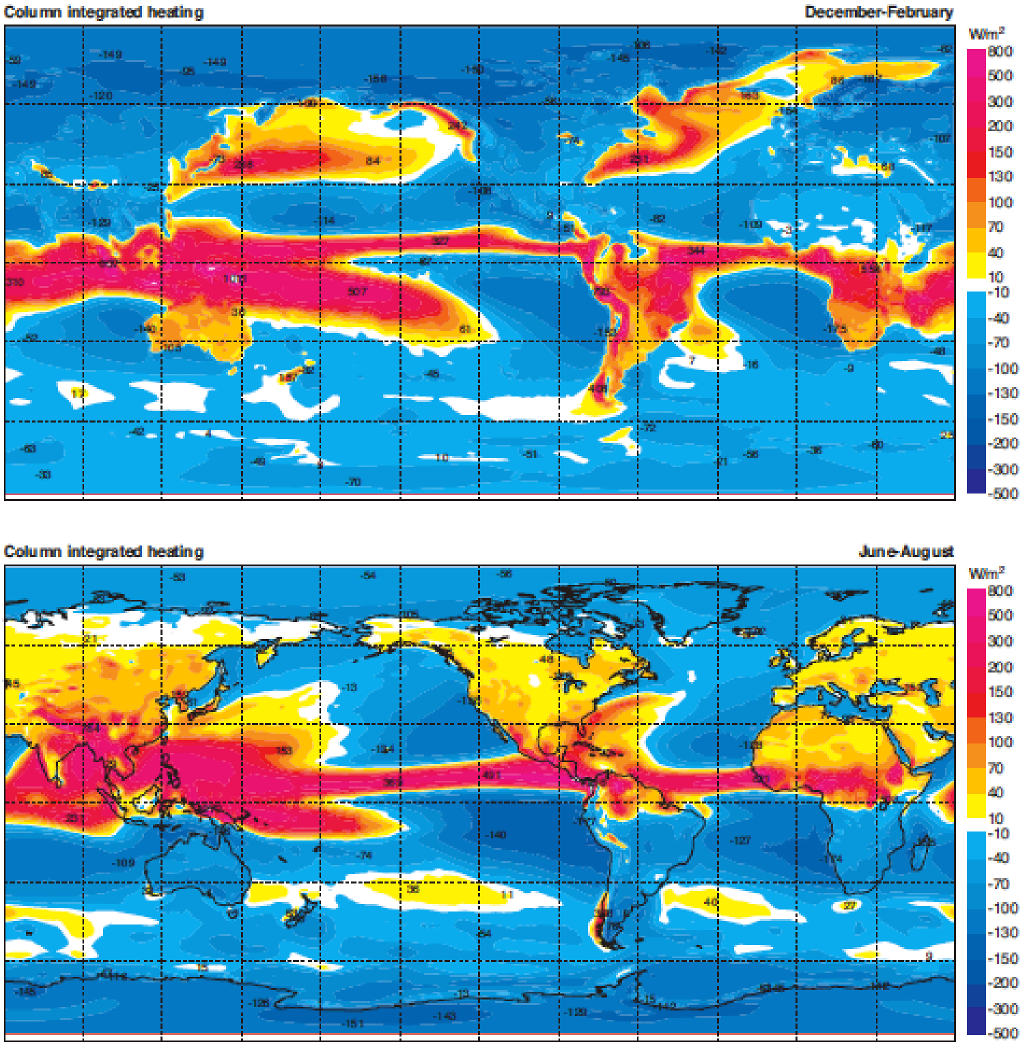

Heating, MAM & SON

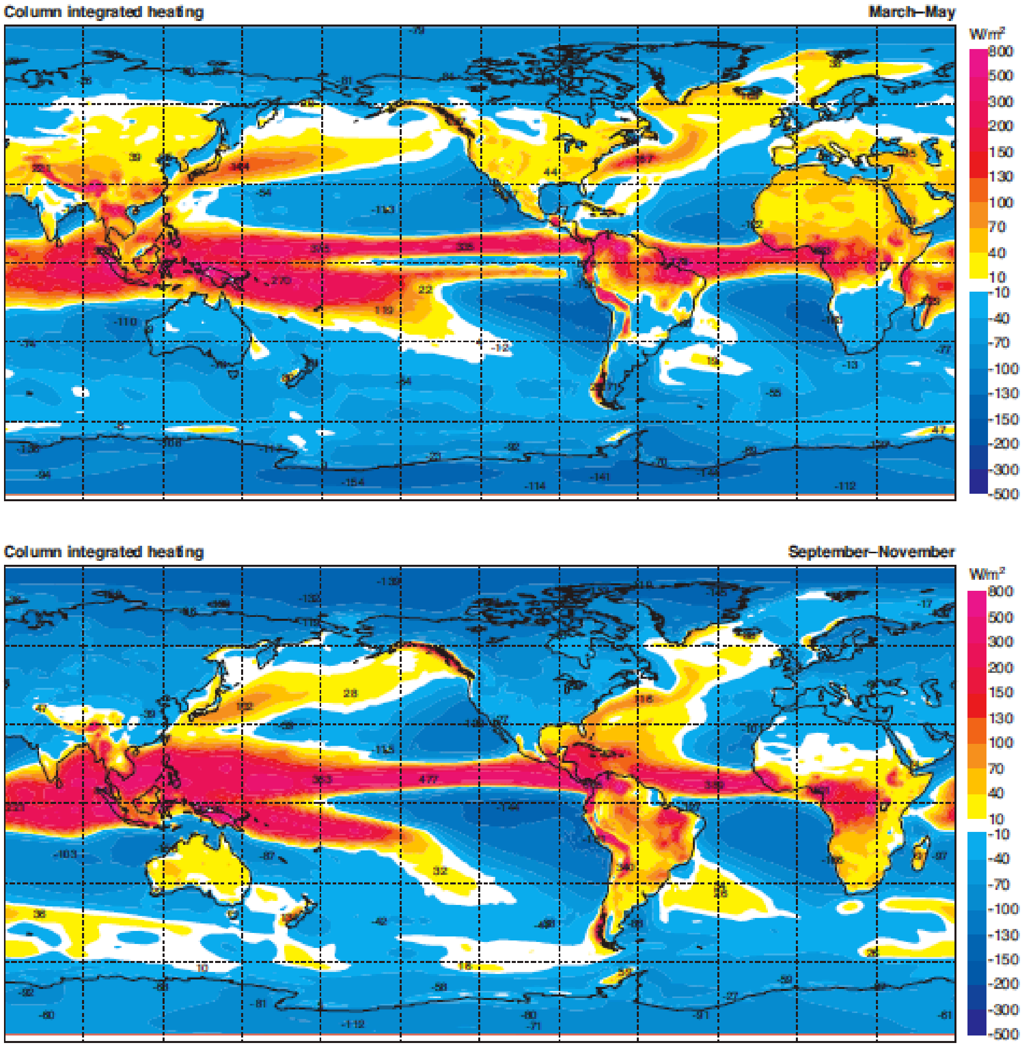

Zonal mean heating and mean meridional stream function, annual mean

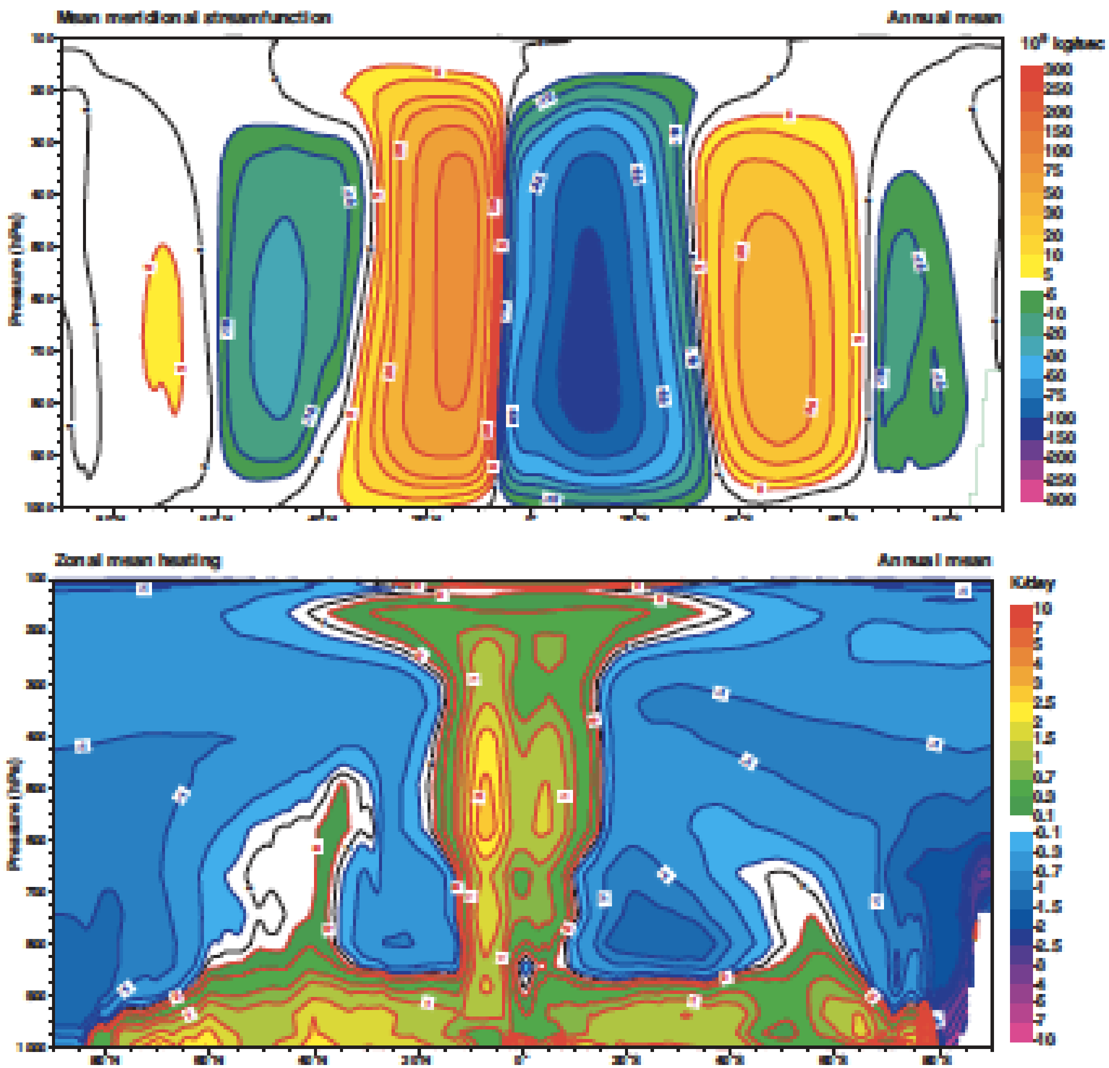

Zonal mean heating and mean meridional stream function, DJF

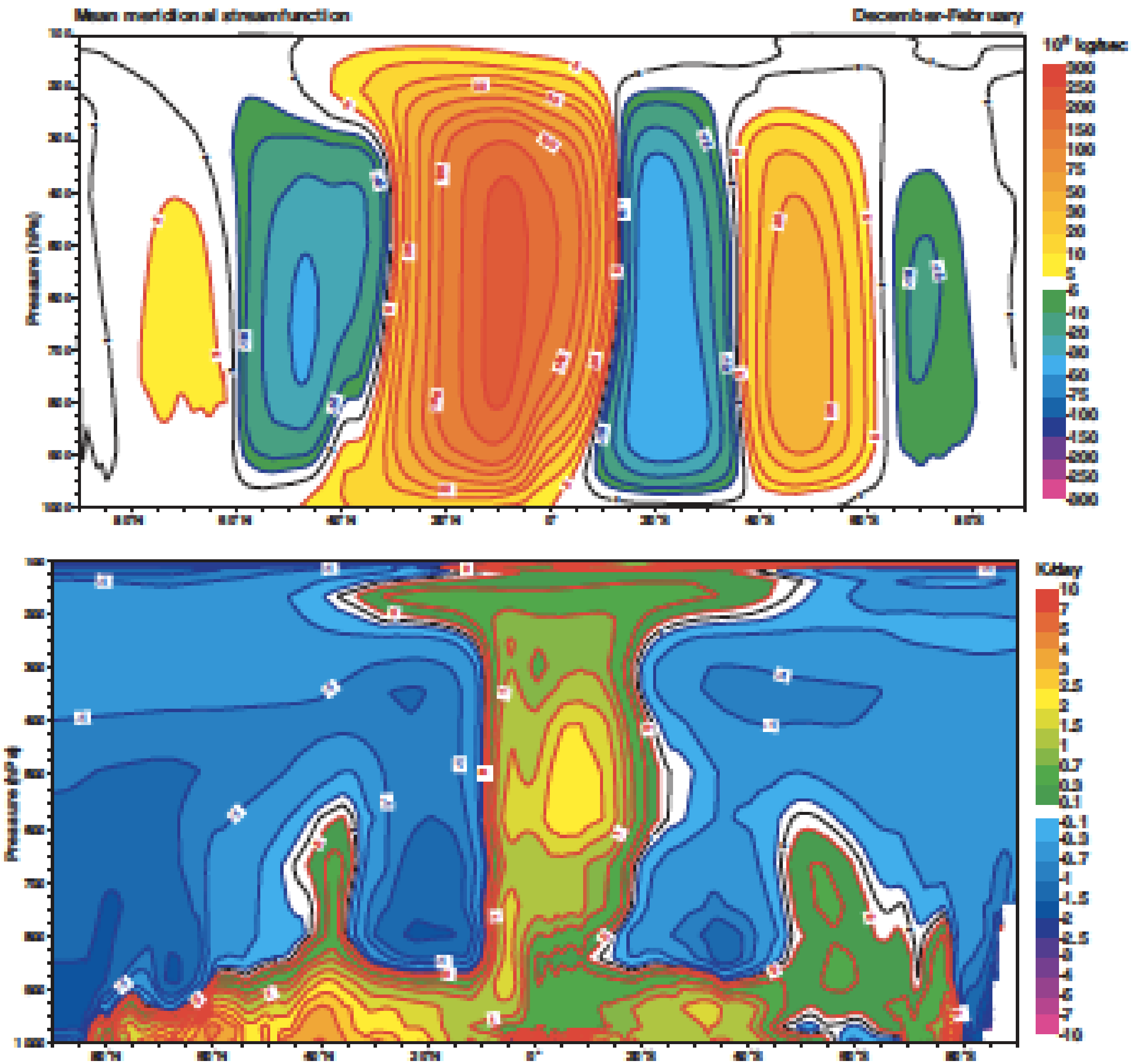

Zonal mean heating and mean meridional stream function, JJA

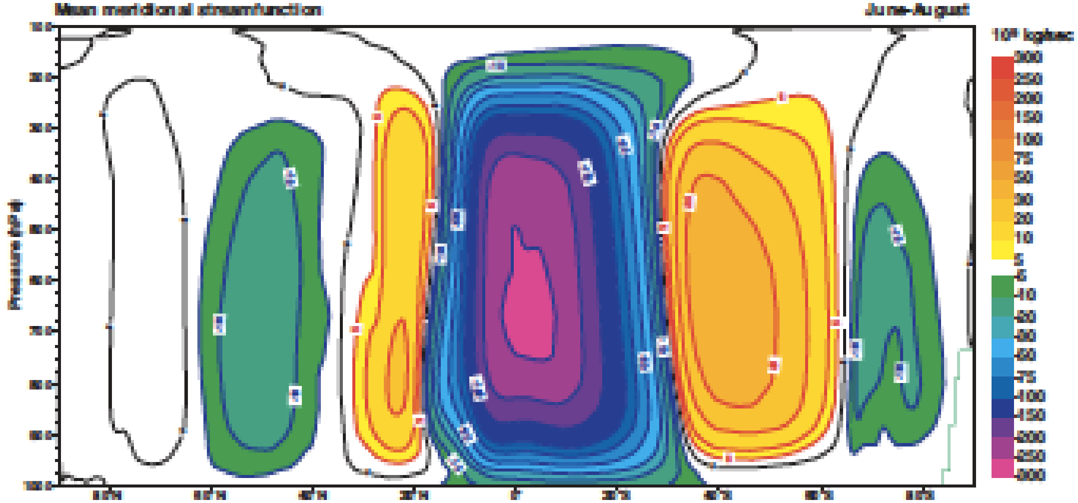

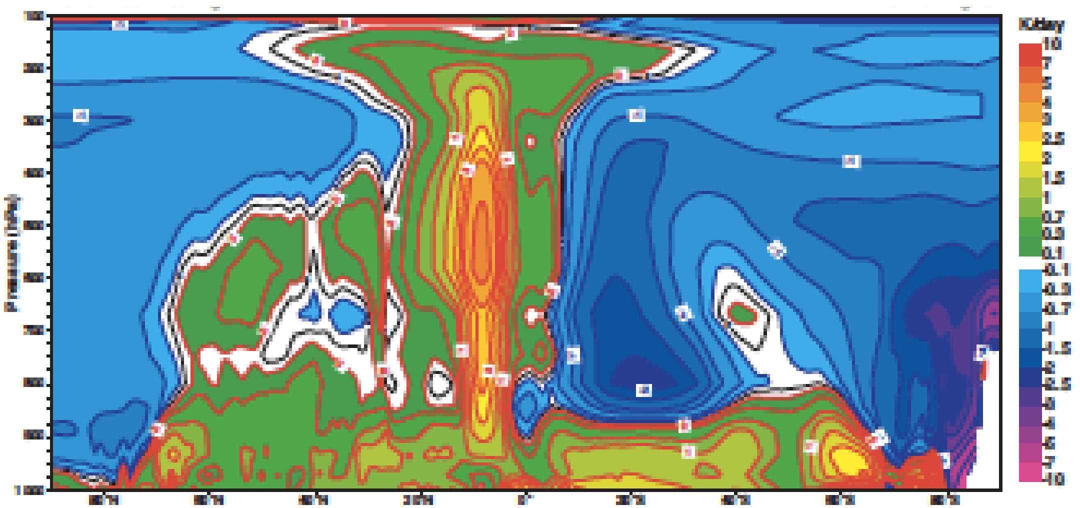

TOA thermal radiation (OLR) and precip, annual mean

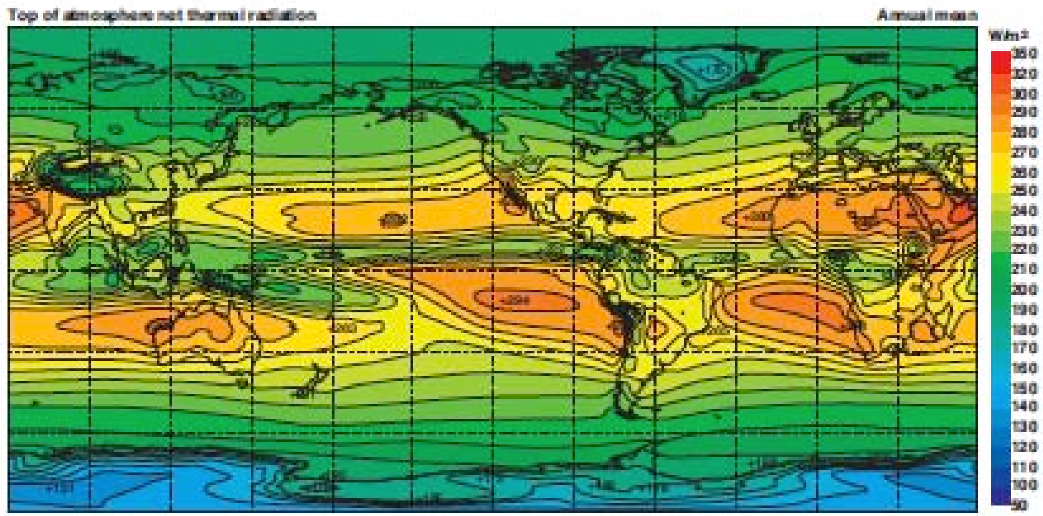

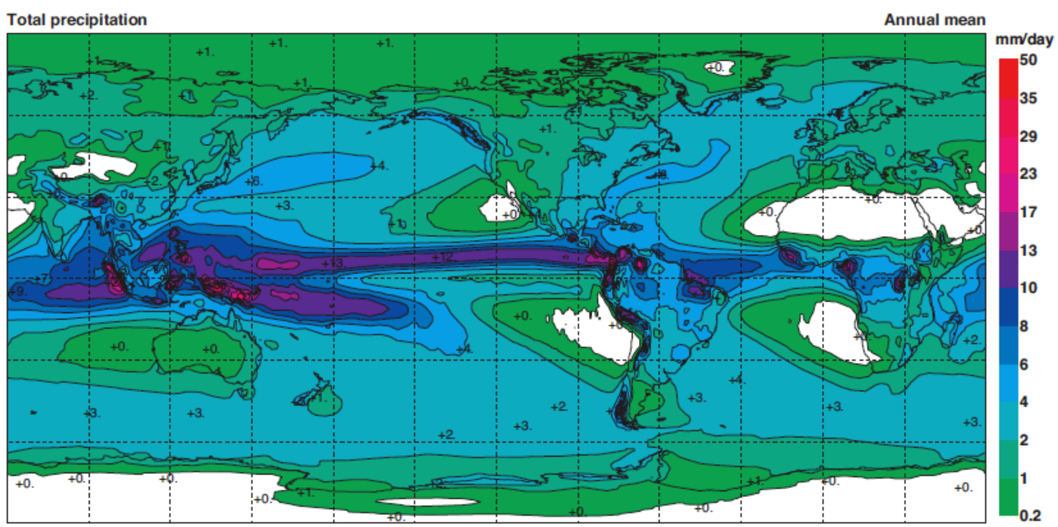

OLR, DJF & JJA

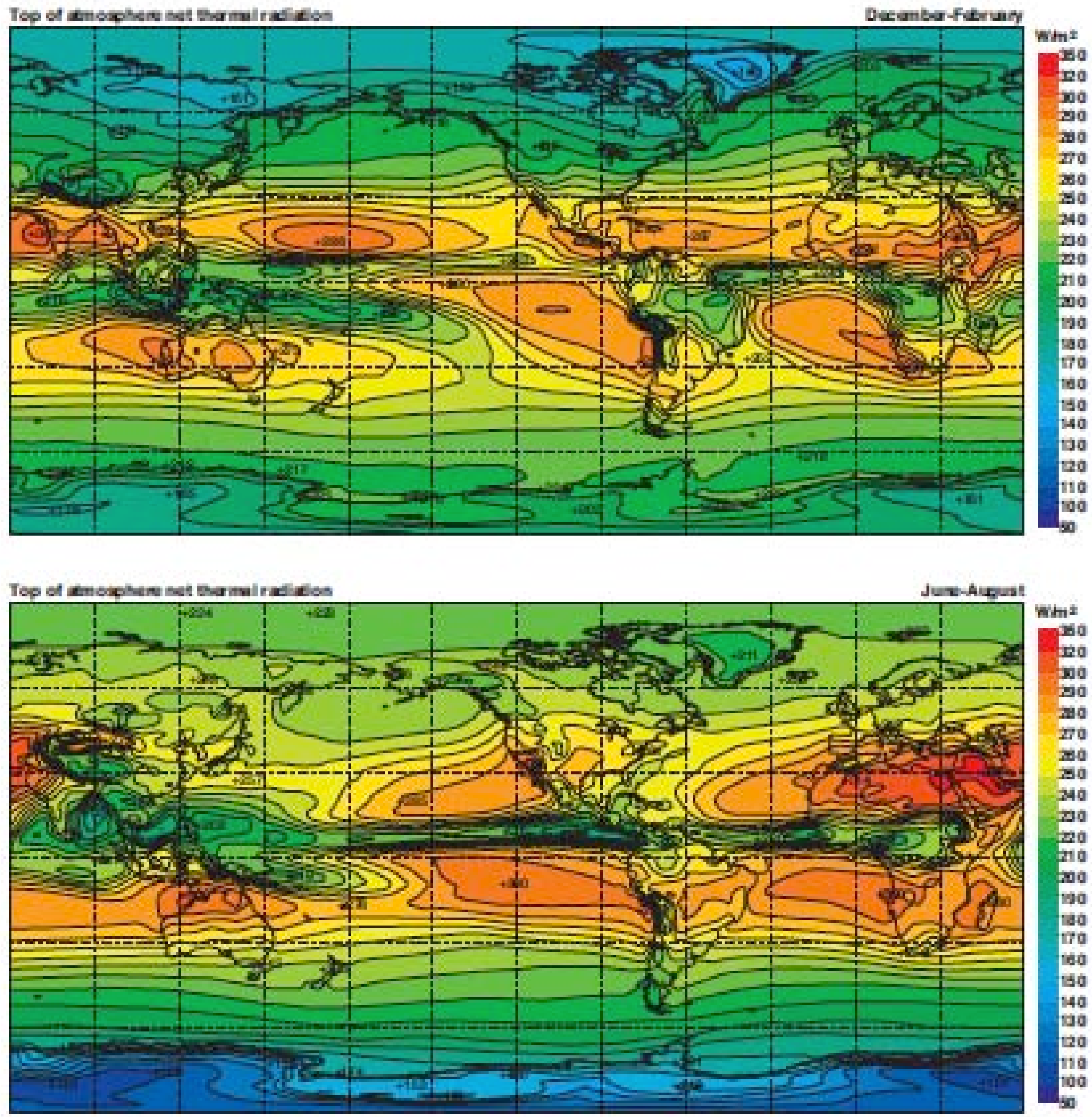
Top of atmosphere net thermal radiation
December-February
W/m²
Top of atmosphere net thermal radiation
June-August
W/m²

OLR, MAM & SON

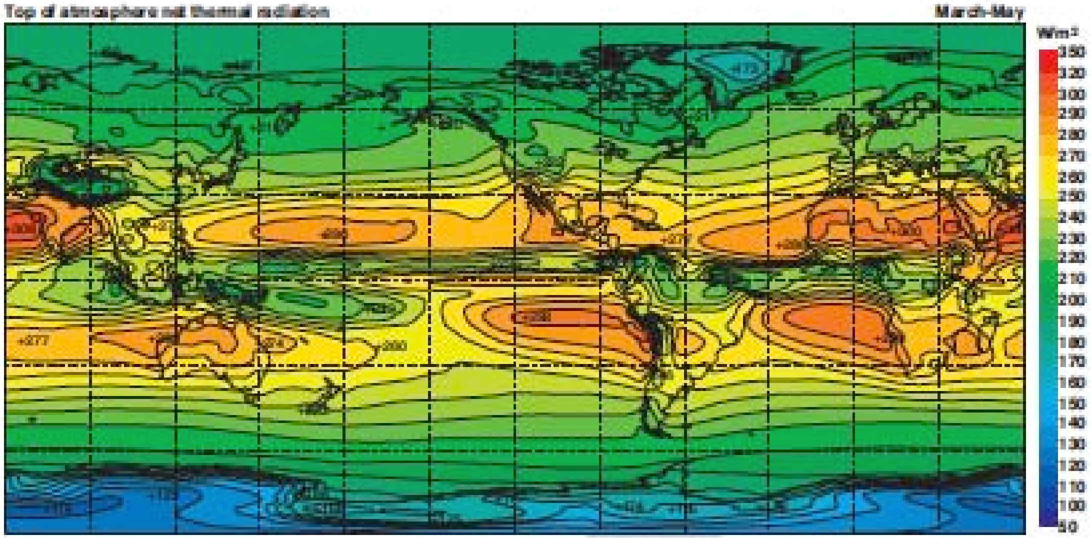
Top of atmosphere net thermal radiation
March-May

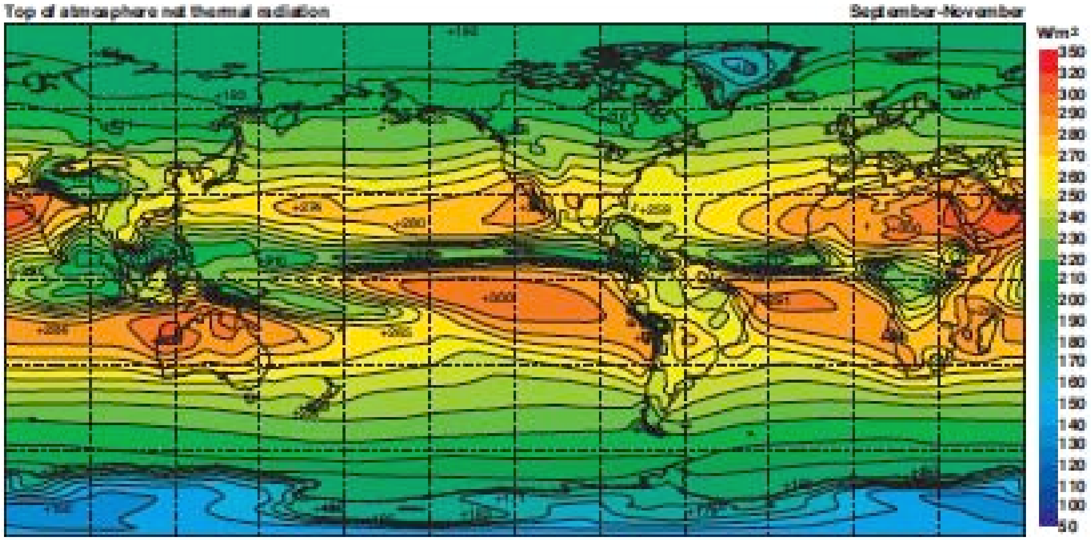
Top of atmosphere net thermal radiation
September-November

Surface latent heat flux and precipitation, annual mean

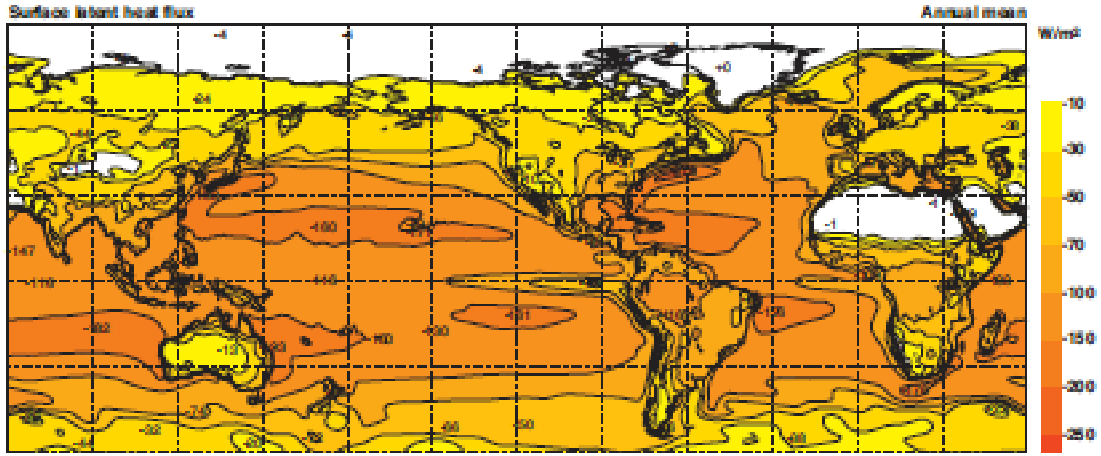

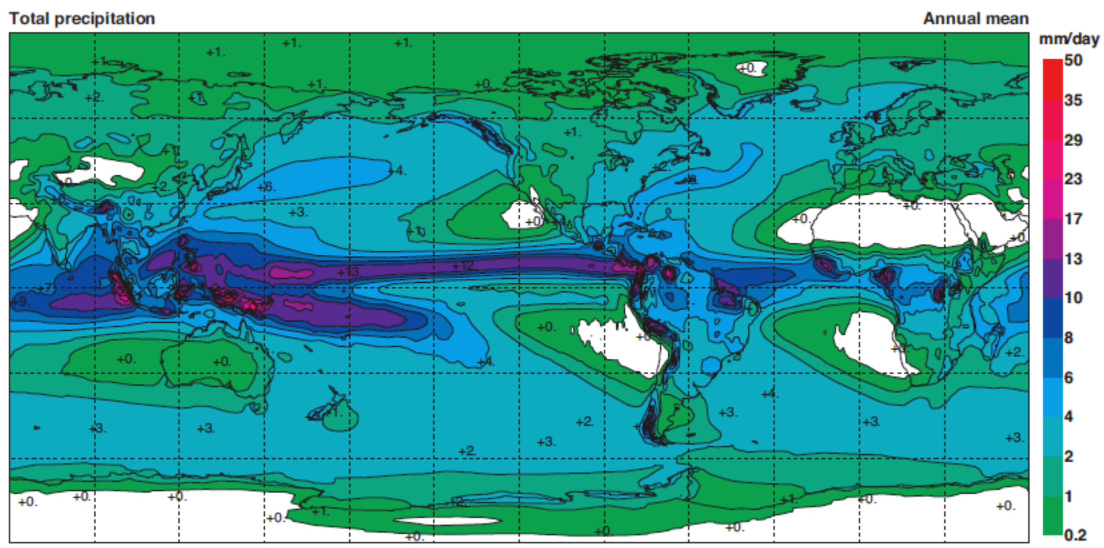

Surface LH flux, DJF & JJA

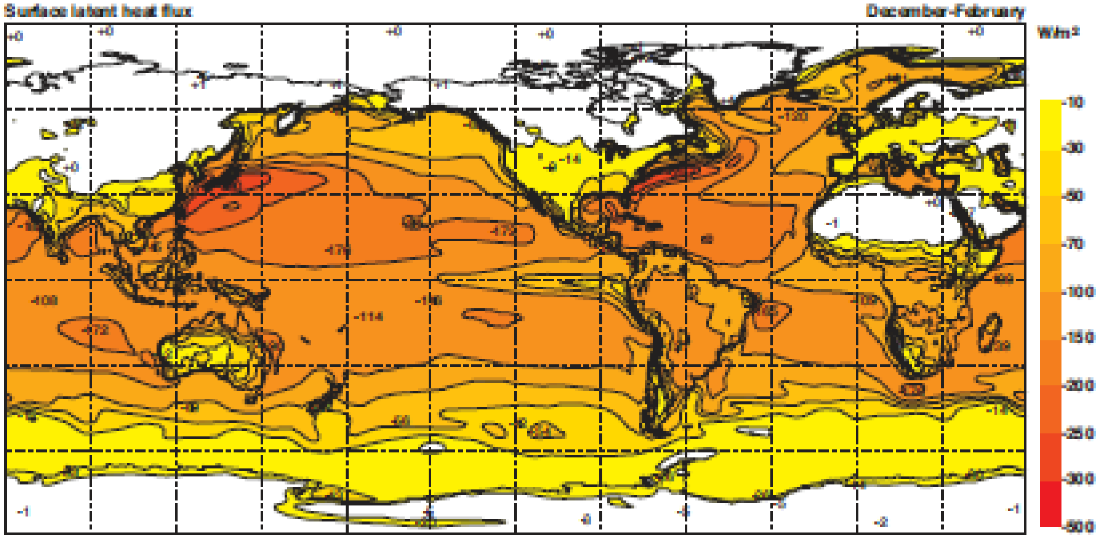

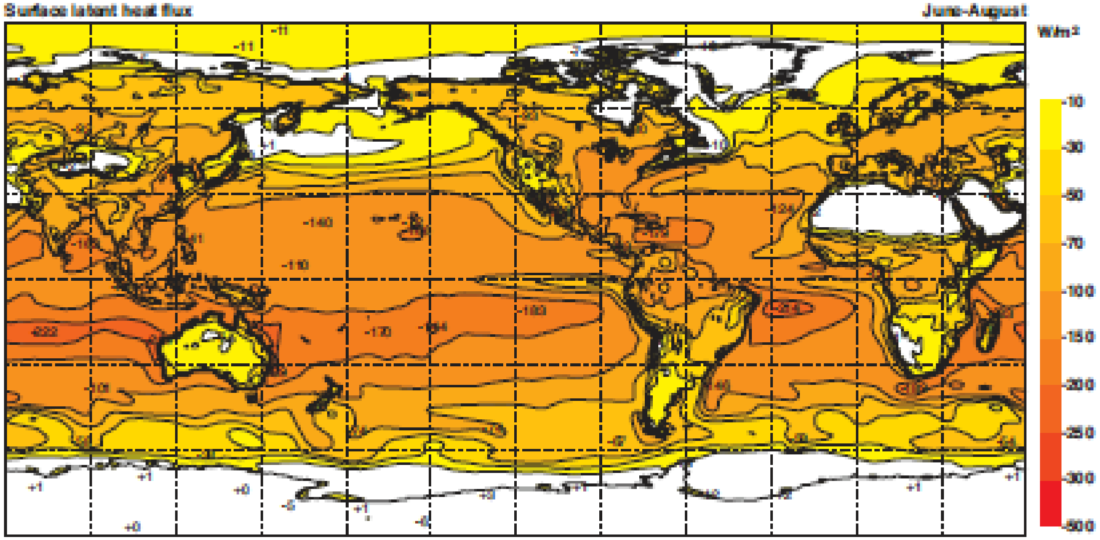

Surface LH flux, MAM & SON

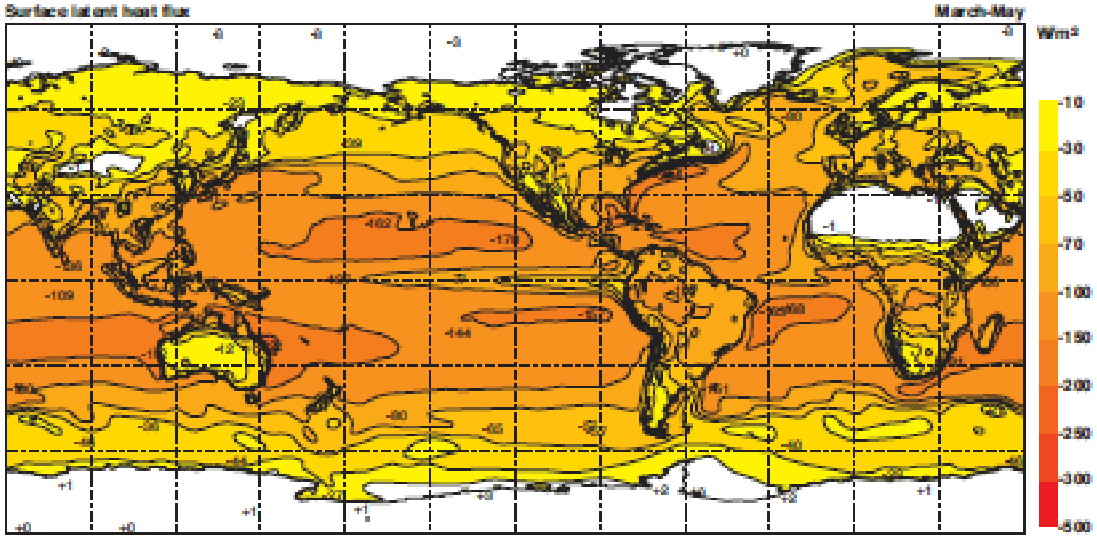

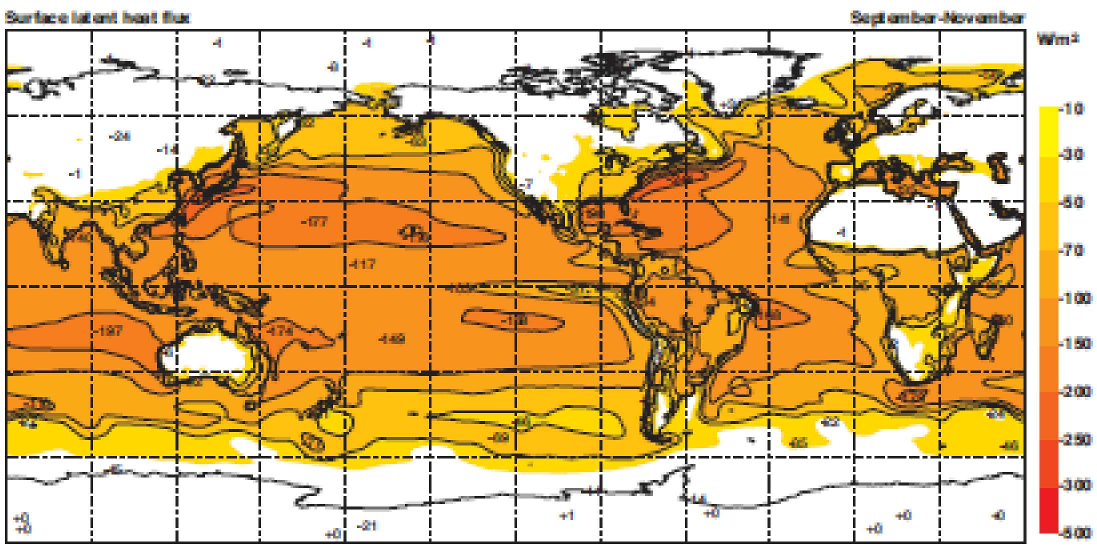

Column-integrated moisture flux and convergence, DJF & JJA

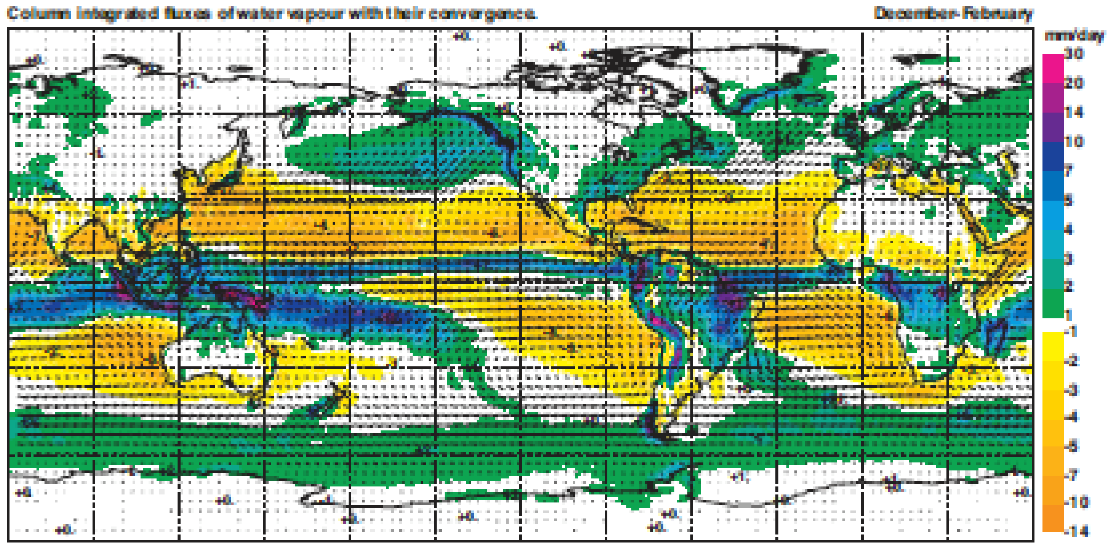

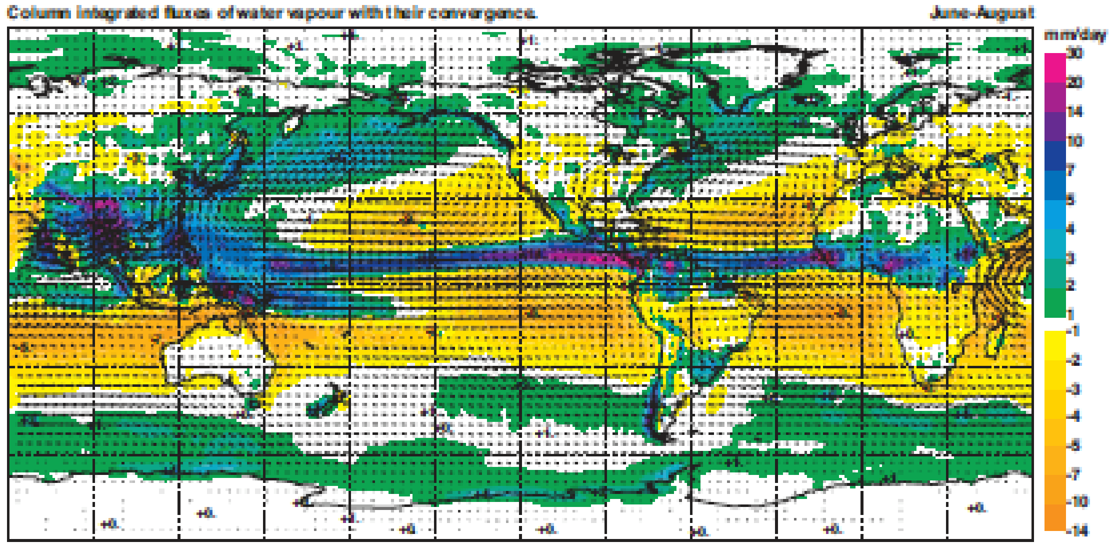

Column-integrated moisture flux and convergence, MAM & SON

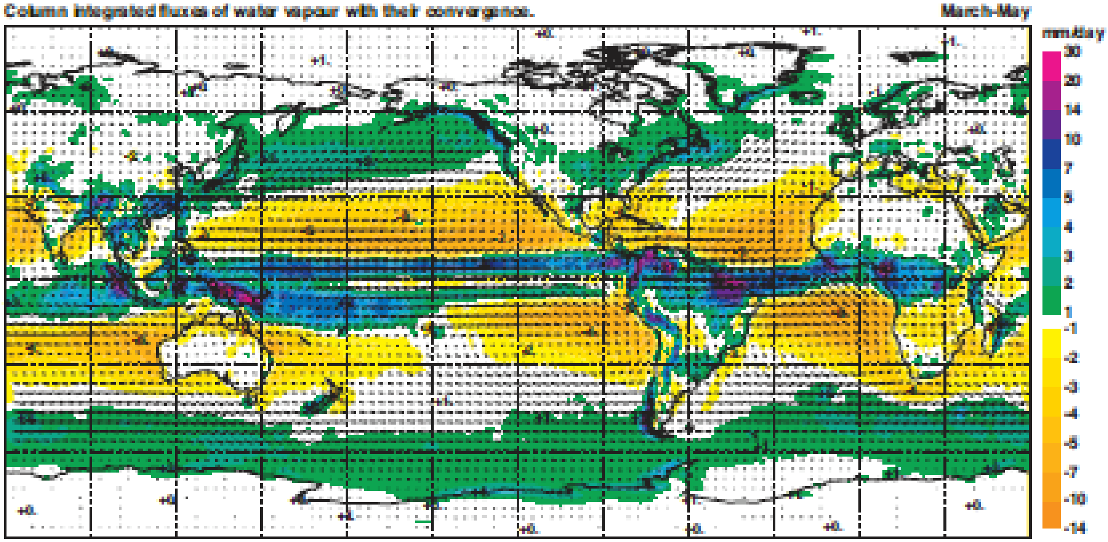

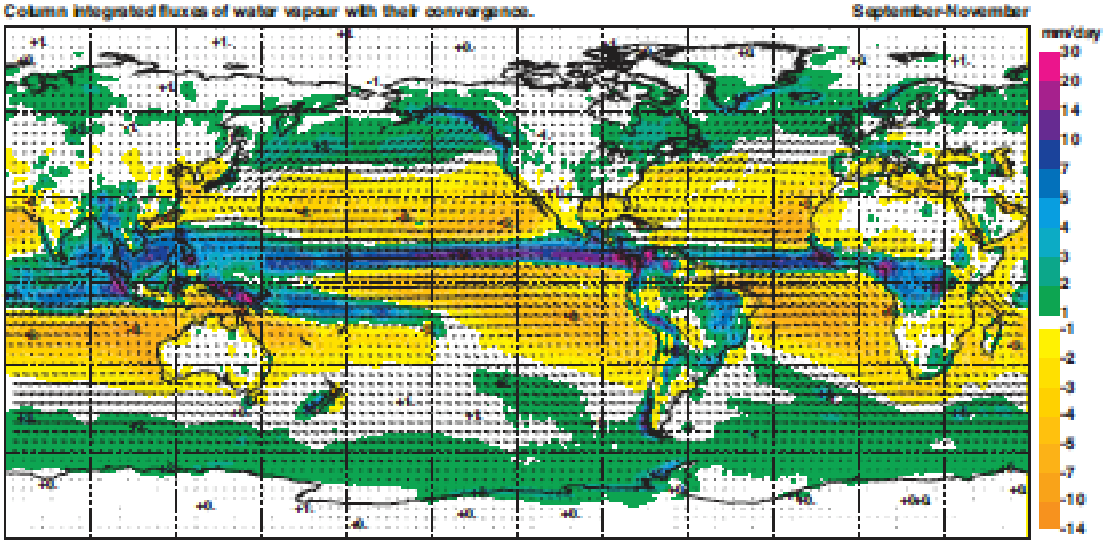

column integrated water vapor & Precipitation, annual mean

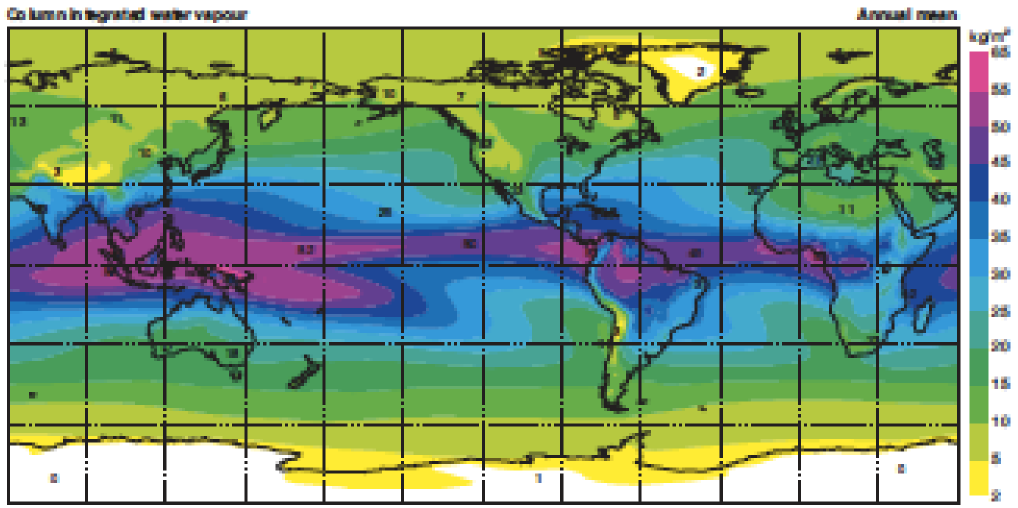

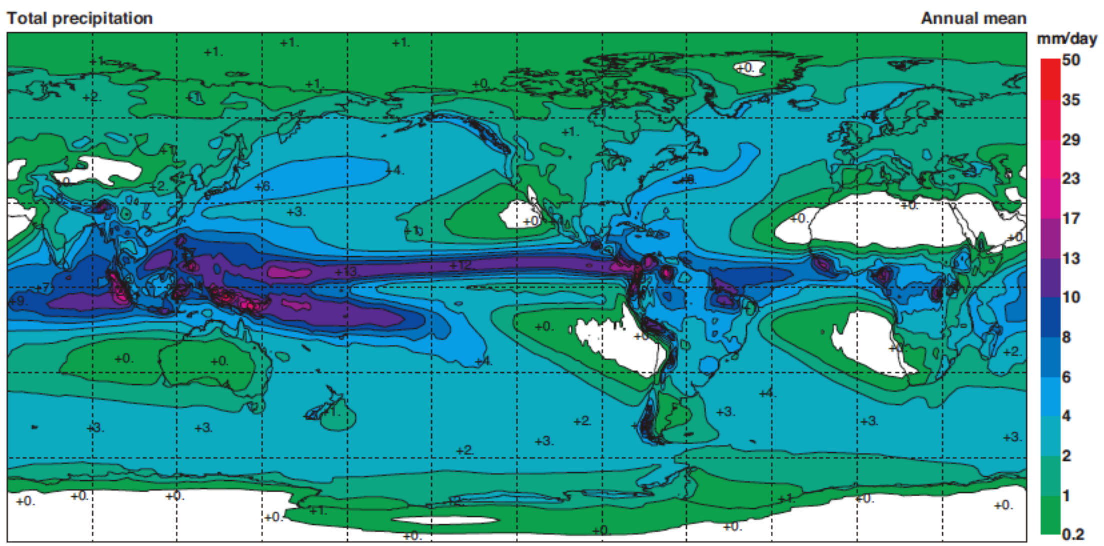

Column water vapor, DJF & JJA

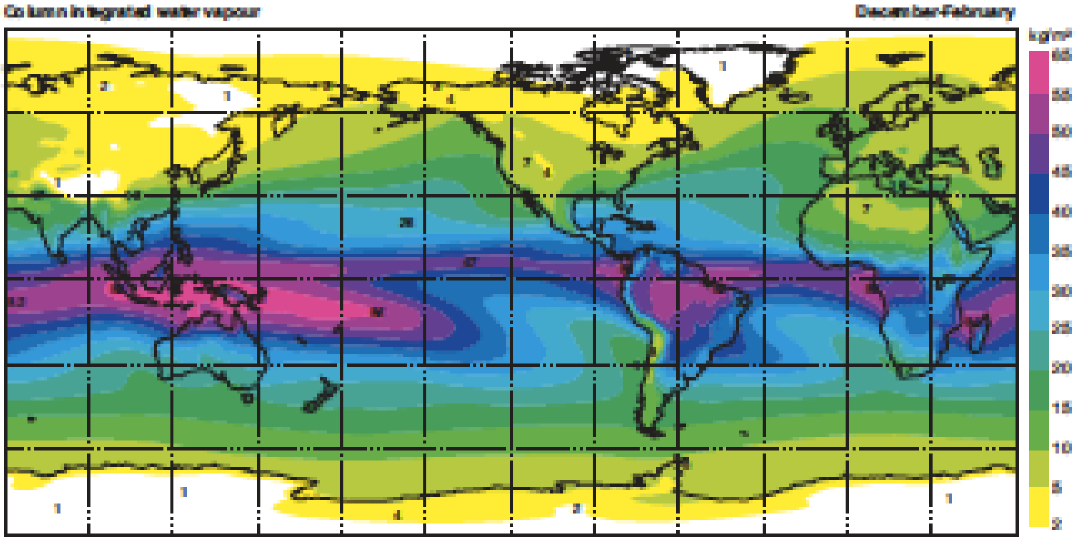

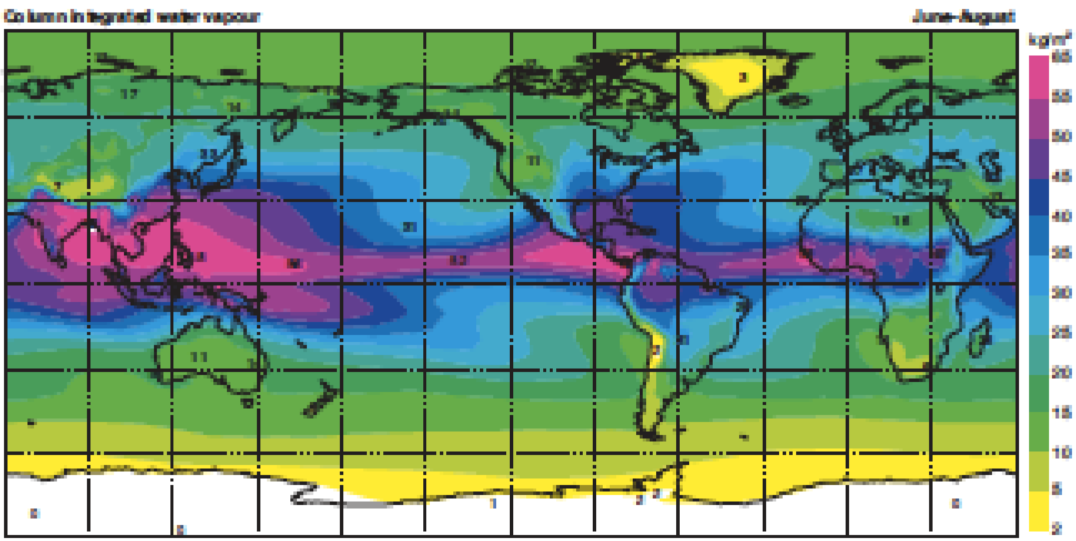

Column water vapor, MAM & SON

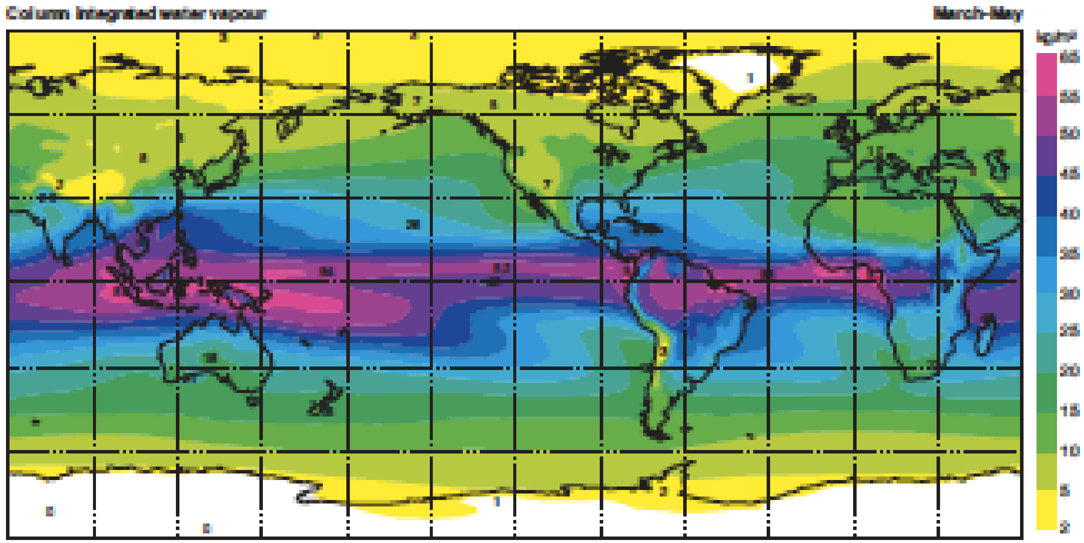

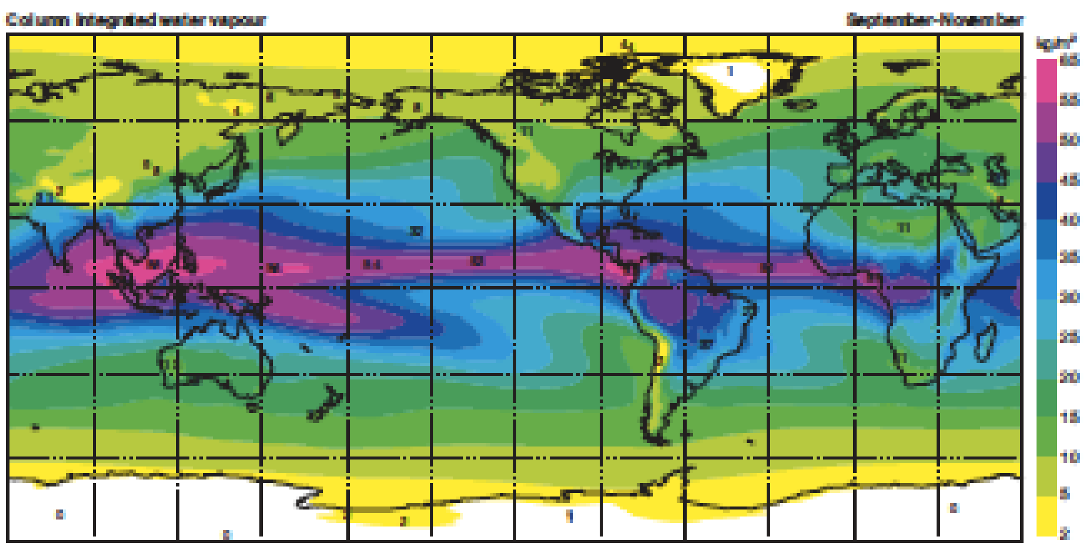

Total surface heat flux (latent+sensible+radiative) annual mean

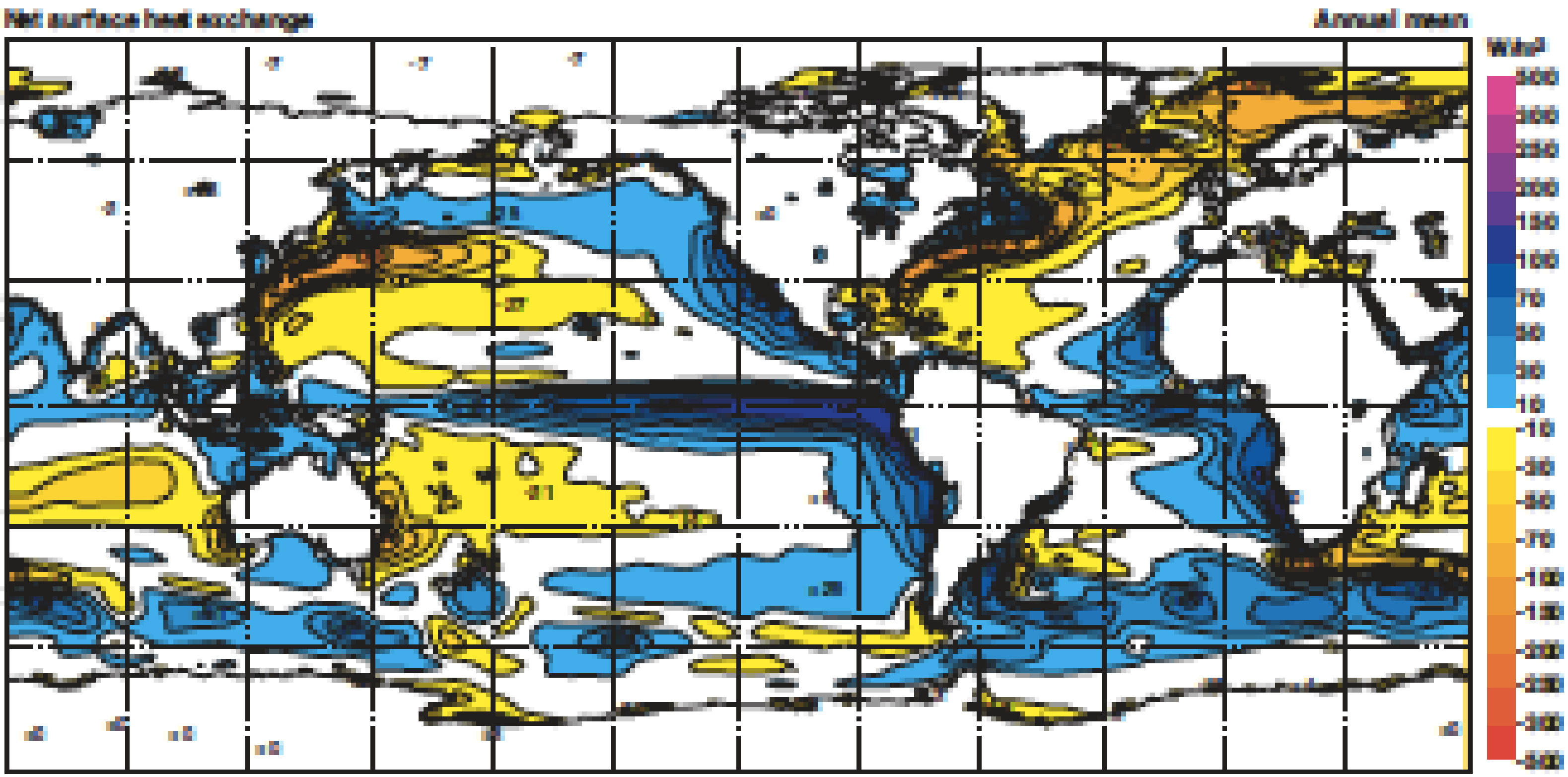

Total surface heat flux (latent+sensible+radiative) DJF & JJA

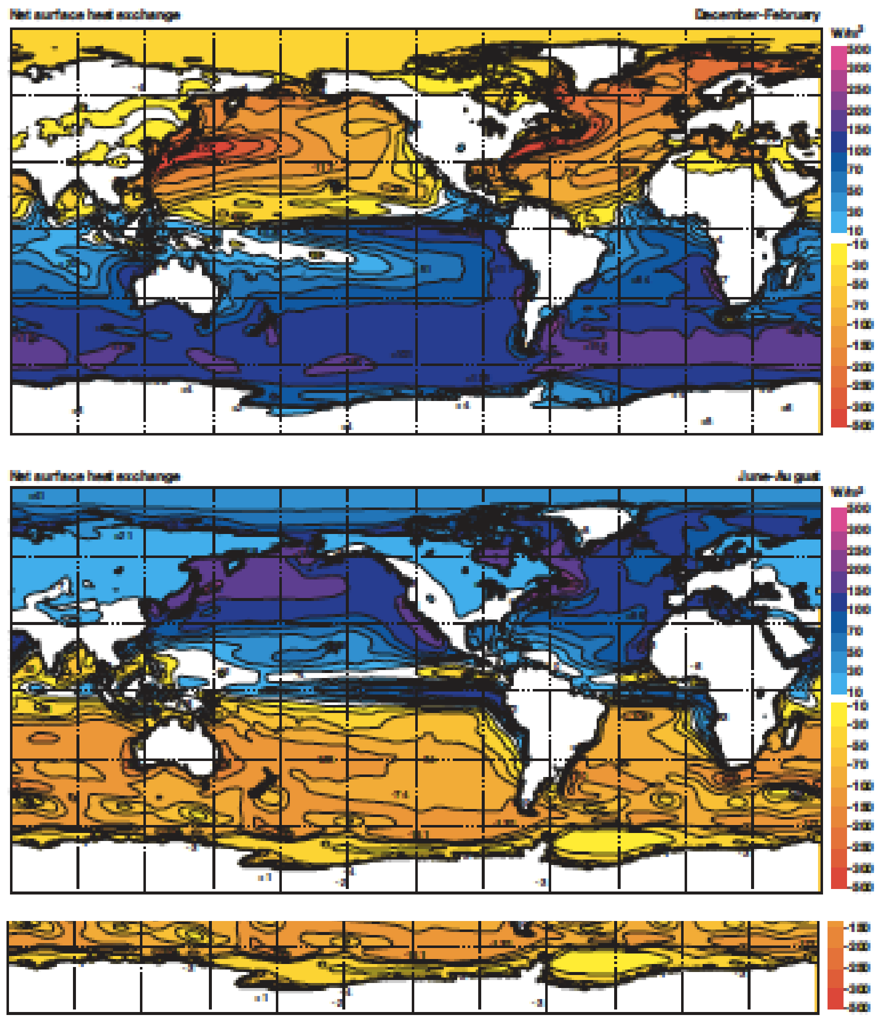

Summary

- Precipitation and vertical motion are tightly linked
- Surface evaporation is much more evenly distributed than precipitation
- The circulation transports water vapor to concentrated precipitation zones
- These are really just statements about the budgets of moisture and dry static energy (or potential temperature)

Summary

- Total surface heat flux is negligibly small over land
- Column-integrated water vapor and precipitation are also tightly associated (*not* a simple budget statement)
- Sea surface temperature and precipitation are also tightly associated (*not* a simple budget statement)
- Free tropospheric temperature has very weak gradients

References 1

- Albrecht, B. A., Jensen, M. P., Syrett, W. J. , 1995: Marine boundary layer structure and fractional cloudiness. J. Geophys. Res., 100, 14209–14222.
- Houze, R. A., Jr., 1989: Observed structure of mesoscale convective systems and implications for large-scale heating. Quart. J. Roy. Met. Soc., 115, 425-461.
- Houze, R. A., Jr., Rutledge, S. A., Biggerstaff, M. I., Smull, B. F., 1989: Interpretation of Doppler weather radar displays in midlatitude mesoscale convective systems. Bull. Amer. Meteor. Soc., 70, 608-619.
- Klein, S. A., Hartmann, D. L., Norris, J. R., 1995: On the Relationships among Low-Cloud Structure, Sea Surface Temperature, and Atmospheric Circulation in the Summertime Northeast Pacific. J. Climate, 8, 1140–1155.
- Rotunno, R., Klemp J. B., Weisman, M. L., 1988: A Theory for Strong, Long-Lived Squall Lines. J. Atmos. Sci., 45, 463–485.
- Smull, B. F., Houze, B. F., 1987: Rear Inflow in Squall Lines with Trailing Stratiform Precipitation. Mon. Wea. Rev., 115, 2869–2889.

References 2

- Sobel, A. H., Yuter, S. E., Christopher S. Bretherton, George N. Kiladis, 2004: Large-Scale Meteorology and Deep Convection during TRMM KWAJEX*. Mon. Wea. Rev., 132, 422–444.
- Stevens, B., 2006: Bulk boundary-layer concepts for simplified models of tropical dynamics. Theor. Comp. Fluid Dyn. 20:5-6, 279-304.
- Takayabu, Y. N., 2006: Rain-yield per flash calculated from TRMM PR and LIS data and its relationship to the contribution of tall convective rain. Geophys. Res. Lett., 33, L18705.
- Webster, P. J., Lukas, R., 1992: TOGA COARE: The Coupled Ocean—Atmosphere Response Experiment. Bull. Amer. Meteor. Soc., 73, 1377–1416.
- Wyant, M. C., Bretherton, C. S., Rand, H. A., Stevens, D. E., 1997: Numerical Simulations and a Conceptual Model of the Stratocumulus to Trade Cumulus Transition. J. Atmos. Sci., 54, 168–192.
- Zipser, E. J., Liu, C., Cecil, D. J., Nesbitt, S. W., Yorty, D. P., 2006: WHERE ARE THE MOST INTENSE THUNDERSTORMS ON EARTH?. Bull. Amer. Meteor. Soc., 87, 1057–1071.